Next Materials 4 (2024) 100217

Contents lists available at ScienceDirect

Next Materials

journal homepage: www.sciencedirect.com/journal/next-materials

Black phosphorus: The rise of phosphorene in 2D materials applications

Raghvendra Kumar Mishra [a,*], Jayati Sarkar [b], Iva Chianella [a], Saurav Goel [c,d], Hamed Yazdani Nezhad [e]

[a] School of Aerospace, Transport and Manufacturing, Cranfield University, MK430AL, United Kingdom
[b] Department of Chemical Engineering, Indian Institute of Technology Delhi, Hauz Khas, Delhi 110016, India
[c] School of Engineering, London South Bank University, London SE10AA, United Kingdom
[d] University of Petroleum and Energy Studies, Dehradun 248007, India
[e] School of Mechanical Engineering, Faculty of Engineering and Physical Sciences, University of Leeds, Leeds, UK

ARTICLE INFO

Keywords:
Black phosphorus
phosphorene
polymer nanocomposites
electronics
energy
storage
Catalysis

ABSTRACT

Few layers Black phosphorus (BP) and phosphorene are two-dimensional (2D) materials renowned for their adjustable bandgaps, high carrier mobility, and anisotropic conductivity, which make them highly promising for applications in the visible and infrared spectrum. The incorporation of these materials into polymer matrices has led to significant advancements in material science, resulting in nanocomposites with enhanced mechanical, electrical, and optical properties. This article provides a thorough analysis of BP/phosphorene polymer nanocomposites, including synthesis techniques (such as exfoliation methods) and manufacturing approaches. Advanced characterisation techniques are utilised to assess the structure, morphology, and properties of these composites. The article highlights the potential applications of these materials in energy storage (e.g., high-capacity batteries), flexible electronics (e.g., bendable displays), environmental sensing, and emerging biomedical fields such as targeted drug delivery. Furthermore, the article discusses potential solutions to tackle the challenges associated with the scalable, cost-effective production and ambient stability of BP/phosphorene, leveraging recent advancements in engineering research. The conclusion outlines future research directions, emphasising the importance of addressing persistent challenges through technological breakthroughs and exploring potential avenues for further advancement.

1. Introduction

Phosphorus (P), the 15th element on the periodic table, plays a vital role in various industrial and biological processes [1]. It exists in numerous allotropes, with black phosphorus (BP) garnering significant interest due to its exceptional electronic and optoelectronic properties [1,2]. Black phosphorus exists in two main phases: alpha (α) and beta (β). α-BP possesses a puckered honeycomb structure similar to graphene, but with a wider bandgap [2]. This wider bandgap makes α-BP attractive for electronic and optoelectronic devices [3,4]. In contrast, β-BP exhibits unique electronic and bonding characteristics, making it well-suited for thermoelectric and energy storage applications [5]. Researchers have employed various techniques to investigate the properties and performance of BP. For example, Latiff et al. [6] explored the cytotoxicity of different phosphorus allotropes, underlining the importance of understanding their impact on biological systems. Kim et al. [7] fabricated high-performance field-effect transistors (FETs) using BP, demonstrating its high carrier mobility and compatibility for device applications.

Abbreviations: 2D, Two-Dimensional; ADF-STEM, Annular Dark-Field Scanning Transmission Electron Microscopy; AFM, Atomic Force Microscopy; $Ag0.25NbSe_2$, Silver Niobium Diselenide; α-BP, Alpha Black Phosphorus; β-BP, Beta Black Phosphorus; BP, Black Phosphorus; CPE, Composite Polymer Electrolyte; CVD, Chemical Vapor Deposition; DFT, Density Functional Theory; EC, Ethylene Carbonate; FET, Field-Effect Transistor; FL-BP, Few-layer Black Phosphorus; LEDs, Light Emitting Diodes; LiCoPO4, Lithium Cobalt Phosphate; MBE, Molecular Beam Epitaxy; μ-ARPES, Micro-focus Angle-Resolved Photoemission Spectroscopy; NASICON, Sodium Super Ion Conductor; P4, White Phosphorus; PC, Propylene Carbonate; PEG, Polyethylene Glycol; PLA, Polylactic Acid; Pox, Phosphorene Oxide; PRS, Polarisation-Resolved Raman Scattering; PRRS, Polarisation-Resolved Raman Scattering-; PVA, Polyvinyl Alcohol; RP, Red Phosphorus; SEM, Scanning Electron Microscopy; SPEs, Solid Polymer Electrolytes; TEM, Transmission Electron Microscopy; TG, Thermogravimetric; TMDCs, Transition Metal Dichalcogenides; TR-ARPES, Time-Resolved Angle-Resolved Photoemission Spectroscopy; UPS, Ultraviolet Photoelectron Spectroscopy; XPS, X-ray Photoelectron Spectroscopy; XRD, X-ray Diffraction.

* Corresponding author.
E-mail address: raghvendramishra4489@gmail.com (R.K. Mishra).

https://doi.org/10.1016/j.nxmate.2024.100217
Received 22 December 2023; Received in revised form 20 April 2024; Accepted 22 April 2024
Available online 3 May 2024

Beyond the fundamental properties discussed earlier, researchers are actively investigating the electronic structure of black phosphorus (BP) using sophisticated experimental and theoretical approaches. This deeper understanding is crucial for optimising its performance in various applications. Wang et al. [8] employed a combined approach of density functional theory (DFT) calculations and optical spectroscopy to analyse the bandgap of BP. This study revealed its key characteristics – a direct bandgap and high light absorption capability – providing valuable insights into its potential for optoelectronic devices. Florian et al. [9] utilised micro-focus angle-resolved photoemission spectroscopy (μ-ARPES) to investigate the electronic structure of ultrathin BP layers. This technique offered a deeper look into its fascinating anisotropic sub-bands, and the researchers established tight-binding parameters for varying thicknesses, providing a more comprehensive understanding of its electronic behaviour. Kwon et al. [10] complemented the experimental findings of Florian et al. by conducting simulations using DFT calculations for nano-sized molecules, including BP. This synergistic approach of combining experimental techniques with theoretical simulations strengthens our understanding of BP's electronic properties at the atomic and molecular levels. Fabio et al. [11] provided a comprehensive overview of time-resolved ARPES (TR-ARPES) techniques. This study sheds light on the ultrafast electron dynamics and out-of-equilibrium electronic structures within various quantum materials, including BP. TR-ARPES offers valuable insights into the behaviour of electrons on ultrashort timescales (femtoseconds), complementing the information obtained from traditional ARPES measurements. Jihang et al. [12] proposed a theoretical model to evaluate the potential of ARPES in addressing fundamental questions within graphene-based moiré superlattices. These artificial materials, formed by stacking layered materials like BP with a twist, have emerged as a promising platform for exploring novel phenomena and manipulating properties of 2D materials [12,13]. While moiré superlattices hold promise for applications like electrocatalytic hydrogen evolution, limitations in theoretical understanding and processing technologies remain challenges [14]. Studies continue to explore sophisticated applications of black phosphorus (BP) and phosphorene by delving into their thermal, mechanical, and functionalisation properties. Han et al. [15] meticulously mapped BP's electronic structure using ARPES, identifying surface resonant states that can influence bulk behaviour. They also demonstrated band structure control through Cs-doping, suggesting potential applications in topological field-effect transistors. Importantly, these surface-resonant states can significantly impact BP-based photodetectors and solar cells. Chen et al. [16] revealed that layers and defects influence BP's high in-plane thermal conductivity, opening avenues for its use in thermal management systems. Meanwhile, Zhou et al. [17] highlighted BP's high Young's modulus and anisotropic stiffness, indicating promise in nanomechanical devices. Bouatou et al. [18] and Su et al. [19] demonstrated that functionalisation – the attachment of chemical groups – can modify BP's electronic and optical properties, offering a way to tailor its behaviour for specific applications. Derived from BP, phosphorene offers exceptional potential for energy conversion and storage. Furthermore, research demonstrates its impressive performance as an anode material in lithium-ion batteries and potential for use in sodium-ion and potassium-ion batteries [20–22]. While, Few-layer BP and phosphorene possess distinct characteristics influencing their suitability for different applications. Few-layer BP's stacked structure and direct bandgap are advantageous for optoelectronics. In contrast, phosphorene's adjustable bandgap, enabling transitions between semiconducting and metallic states, offers versatility for electronic applications. Although few-layer BP exhibits higher carrier mobility and thermal conductivity, phosphorene's properties can be optimised through structural engineering [23,24]. Few-layer BP's strong electronic anisotropy provides advantages for electronics and optoelectronics, including high in-plane carrier mobility, tailorable bandgap, strong light-matter interactions, and polarisation-sensitive device characteristics [22]. Meanwhile, surface modification plays a crucial role in tailoring the properties of both few-layer BP and phosphorene. It allows for customisation of electronic properties, enhanced stability, improved biocompatibility, and even catalytic activity, particularly in phosphorene [8,23,25]. Fig. 1 offers a concise overview of the structures, properties, and applications of BP and phosphorene, emphasising their potential in electronics, optoelectronics, and energy storage.

2. Background and scope of black phosphorus and phosphorene

Black phosphorus (BP), discovered in the early 1900 s, has captivated researchers for its potential in electronic and optoelectronic applications since the 1960 s. The development of exfoliation techniques in the early 2010 s enabled the creation of thin layers of BP, known as few-layer BP. Notably, Bridgman's work played a significant role in the development of scalable production methods for BP. In 2014, a significant breakthrough occurred with the introduction of phosphorene, a single-layer derivative of BP, opening new avenues for device development [26]. BP is one of the most stable phosphorus allotropes at high temperatures and pressures [27]. Its distinctive crystal structure exhibits two key directional characteristics: zigzag and armchair. Each layer comprises phosphorus atoms arranged in zigzag chains with a bond angle of approximately 99° and a bond length of 2.18 Å. Weak van der Waals forces hold the layers together, with an interlayer spacing of about 5.3 Å [28]. Unlike the flat layers of graphite and graphene, BP's layers have a corrugated or puckered shape. This unique structural characteristic contributes to the exceptional electronic and mechanical properties that distinguish BP and phosphorene from other two-dimensional materials. Phosphorene, a single-layer derivative of BP, possesses a two-dimensional honeycomb lattice structure with characteristic ridges on two parallel planes [29,30]. Fig. 2 provides a schematic representation of the crystal structures of BP and phosphorene for a comparison.

Beyond their exceptional structure, black phosphorus (BP) and phosphorene exhibit remarkable potential in various applications. Their favourable electrochemical properties and high theoretical specific capacity make them promising candidates for advanced lithium-ion batteries and efficient photovoltaic devices [32]. Notably, their sensitivity to chemical and physical stimuli allows for the development of sensors for gas, pressure, strain, and humidity detection [33]. Furthermore, their unique optical properties open doors for applications in imaging and optical sensing. Biomedical research is actively exploring the potential of BP and phosphorene in drug delivery systems, bioimaging, and tissue engineering, where biocompatibility is paramount [34]. Additionally, their electronic structure and high surface area make them promising catalysts for clean energy processes like hydrogen evolution and oxide reduction reactions [35]. Composites combining BP or phosphorene with polymers, metals, and metal oxides offer exciting possibilities for further enhancing properties and introducing new functionalities. These combinations can lead to significant improvements in mechanical, electrical, and optical performance [36]. Understanding the properties and applications of BP and phosphorene necessitates the use of sophisticated characterisation techniques. X-ray diffraction (XRD) provides valuable insights into crystal structure, layer thickness, and orientation. Transmission electron microscopy (TEM) offers atomic-scale imaging and defect analysis capabilities. Raman spectroscopy aids in determining the number of layers through analysis of vibrational properties. Field-effect transistors (FETs) are crucial tools for measuring electrical transport properties. Additional techniques like scanning tunnelling microscopy (STM), photoluminescence (PL) spectroscopy, X-ray photoelectron spectroscopy (XPS), ultraviolet photoelectron spectroscopy (UPS), and capacitance-voltage (C-V) measurements can provide further comprehensive information [37,38]. It's crucial to recognise that bulk BP, few-layer BP, and phosphorene possess distinct properties. Each form has a unique structure, bandgap, carrier mobility, stability profile, and set of suitable applications. Phosphorene, despite its lower stability, boasts the highest carrier

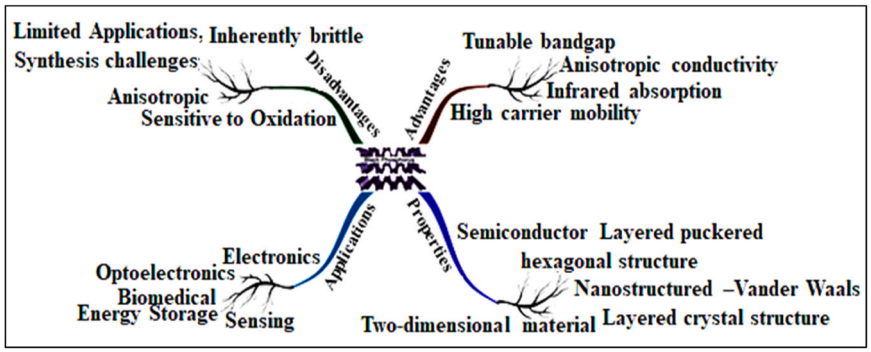

Fig. 1. Black Phosphorus: A Versatile Material for Cutting-Edge Applications.

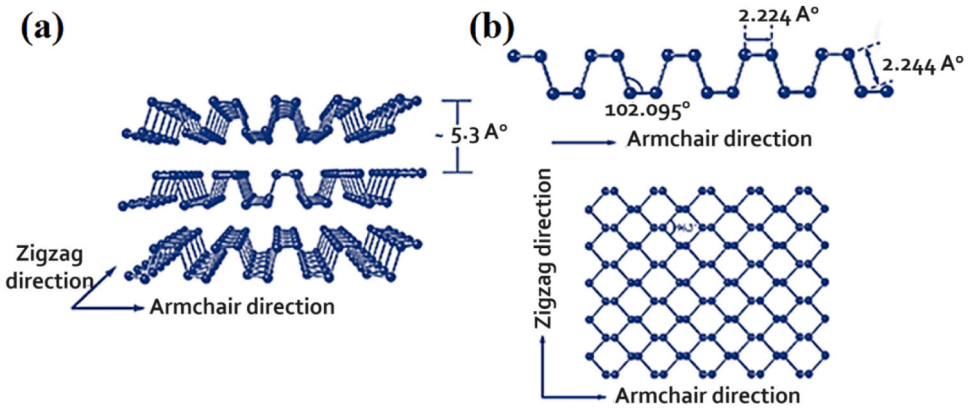

Fig. 2. Schematic representation of a) black phosphorus, b) phosphorene crystal structure [31].

mobility and a tuneable bandgap, making it attractive for optoelectronic applications. Few-layer BP offers a well-balanced combination of performance and stability, surpassing bulk BP in some aspects. Bulk BP, being the most stable form, finds applications in various fields, as summarised in Table 1.

2.1. Synthesis methods of black phosphorus

The synthesis of black phosphorus (BP) and its single-layer derivative, phosphorene, involves various methods relying on either red phosphorus (RP) or white phosphorus (P4) precursors. Each method offers advantages and limitations in terms of the material's desired properties and applications [32]. Fig. 3 provides a visual overview of these synthesis routes. High-energy ball milling method efficiently produces BP, allowing optimisation of milling conditions to avoid thermal degradation. Post-milling treatments can further enhance BP crystallinity and purity [41–43].

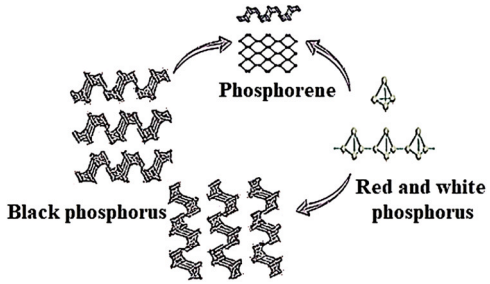

Fig. 3. Synthesis route for black phosphorus and phosphorene.

Chemical vapor transport (CVT) produces high-quality BP single crystals with controlled properties [44–46]. Wet-chemical methods

Table 1
Black Phosphorus, Few-Layer Black Phosphorus, and Phosphorene comparison [39,40].

Property	Black Phosphorus	Few-Layer Black Phosphorus	Phosphorene
Structure	Layered material with puckered honeycomb lattice	Stacked layers of black phosphorus	Single-layer BP sheet
Thickness	Bulk material or few layers	Typically, 2–10 layers	Monolayer
Bandgap	Tuneable from 0.3 eV to 2.0 eV	Tuneable from 0.3 eV to 1.88 eV	1.2–2.0 eV
Carrier Mobility	Up to 1000 cm^2/Vs at room temperature	640–700 cm^2/Vs for monolayer BP; 4800–6400 cm^2/Vs for five layers	10,000–26,000 cm^2/Vs at room temperature
Electrical Conductivity	High	Lower than bulk BP but significant	Highest among the three materials
Stability	More stable than phosphorene; remains stable at atmospheric conditions for a few months	Less stable than bulk BP; medium reactivity and air instability	Less stable than bulk BP and few-layer BP; highest reactivity and air instability
Thermal Conductivity	Good heat conductor with high anisotropy	Increases with thickness; exhibits anisotropy	Highest among the three materials with high anisotropy
Applications	Photodetectors, solar cells, field-effect transistors, energy storage, thermal management	Similar applications to bulk BP, but with reduced performance	Optoelectronic devices, energy storage, sensors, catalysis, biomedical applications

employs reducing agents for molecular-level control over BP synthesis, allowing customisation of its morphology and structure [47,48]. Bridgman method achieves high-quality BP crystals, but environmental and health risks due to mercury use pose concerns [49–51]. Melting method produces high-quality BP under high pressure, but faces challenges related to equipment costs, energy consumption, and safety [52, 53]. Low-temperature solution synthesis generates few-layer phosphorene or BP with tailored optical and electronic properties [53–55]. Mechanical exfoliation is a simple, cost-effective way to produce few-layer or monolayer BP flakes [56]. Chemical vapor deposition (CVD) enables controlled doping of large-area BP films, but requires specialised equipment and conditions [57]. Liquid-phase exfoliation (LPE) is scalable production of high-quality BP nanosheets, but limitations exist in generating large-area films [58]. Direct phosphorylation allows BP growth on various substrates but introduces complexities and potential quality issues [59]. Solvothermal-assisted LPE combines solvent dispersion with high-temperature treatment for thickness control and scalability [60]. One-step hydrothermal process offers a simple, cost-effective way to create high-quality BP crystals suitable for electronics and optoelectronics [41]. BP undergoes phase changes under high pressure, exhibiting superconductivity at extreme conditions [61]. The optimal synthesis approach depends on desired properties, resources, and equipment [55]. For example, vapor deposition allows growth on various substrates, while pressure quenching can yield crystals for fundamental research. Specific application necessitates careful method selection. Mechanical exfoliation suits biosensors, drug delivery, and tissue scaffolds [62]. CVD is ideal for biocompatible polymers films [63]. LPE produces nanosheets for bioimaging and targeted therapy [64], while direct phosphorylation can improve biosensor performance [65,66]. Table 2 offers a useful comparative evaluation of synthesis techniques.

Table 2
Comparison of Different Synthesis Methods for Black Phosphorus.

Method	Parameters	Key Findings and Additional Notes	Ref.
Chemical Vapor Transport (CVT)	High temperature, vacuum conditions, sealed quartz tube	High-temperature, vacuum conditions, sealed quartz tube for large BP crystal synthesis. Cooling rate affects crystal size.	[67]
Wet-Chemical Methods	Temperature, concentration, pH	Precise control needed for solid formation. Simple methods face yield and purity challenges.	[68,69]
Bridgman's Method	Temperature gradient, controlled	Requires temperature gradient, controlled atmospheres, expensive equipment.	[70]
Modified Bridgman's Method	Temperature gradient, rate of crucible	Temperature gradient crucial; slow crucible movement enhances crystal growth. Dopant control challenging.	[71]
Mercury Catalysis	Mercury dosage, catalyst type	High yield, large crystal size with mercury catalysts. Alternatives reduce environmental hazards.	[38]
Liquid Bismuth Method	High pressure, high temperature, slow cooling rate, purity of bismuth and phosphorus, safety protocols	High-pressure, high-temperature environment. Slow cooling, purity crucial. Bismuth toxicity requires safety measures.	[72]
Melting Method with High Isobaric Pressure	Pressure, temperature, cooling rate	High-quality BP crystals with precise temperature control. Expensive equipment, energy-intensive process.	[70]
One-Step Hydrothermal Method	Temperature, pressure, EDA concentration, pH control, safety measures	Low-temperature BP synthesis using ethylenediamine. pH, EDA concentration critical. Safety precautions necessary.	[73]
High-Energy Ball Milling	Ball to Powder Ratio (BPR), milling speed, milling time, milling atmosphere	BPR, milling speed, and time affect particle properties. Inert atmospheres prevent oxidation. High conversion yields but may compromise crystallinity.	[67, 74–76]
High Isobaric Pressure Melting Method	Pressure, temperature, cooling rate	High-pressure equipment essential for large BP crystal growth. Precise temperature control needed. Slow cooling rates preferred.	[64,67]
CVT Method (Sn/I2/red-P system)	Temperature, sealed quartz tube	Simplified purification, high crystallinity BP. Two-step heating process. Mechanism not fully understood.	[59,77]
CVT Method (Sn/SnI4/red-P system)	Temperature, precursor synthesis	Cost-effective, challenges in precursor synthesis.	[77]
Nilges's CVT Approach	Trace minerals, impurities	Trace minerals enhance synthesis but may introduce impurities.	[77]
High-Pressure White Phosphorus Preparation	Pressure, temperature	Utilises high-pressure equipment for BP synthesis.	[74–76]

2.2. Synthesis methods of phosphorene

Phosphorene, a single-layer derivative of black phosphorus (BP), possesses exceptional electronic, optical, and mechanical characteristics that hold immense potential for various applications [78]. To fully realise this potential, efficient and scalable synthesis of high-quality phosphorene is paramount. Black phosphorus (BP), the most stable allotrope of phosphorus, adopts a layered structure consisting of puckered honeycomb lattices. Within each layer, individual phosphorus atoms covalently bond with three neighbours [39,40]. Bulk BP behaves as a semiconductor with a narrow bandgap, while phosphorene exhibits a wider bandgap that depends on its thickness. Notably, the bandgap transitions from indirect to direct as the number of layers decreases [79]. Additionally, phosphorene boasts high carrier mobility, a tuneable bandgap, and pronounced in-plane anisotropy – properties that make it highly attractive for applications in nanoelectronics, optoelectronics, sensing, and energy conversion [50]. The compelling properties of phosphorene, particularly its high carrier mobility and strong ultraviolet (UV) absorption, make it an ideal candidate for optoelectronic devices. To meet the growing demand for this material, researchers have developed a diverse range of synthesis methods [80]. These methods can be broadly categorised into two main approaches: top-down and bottom-up. As illustrated in Fig. 4, the choice of synthesis method significantly impacts the properties and performance of phosphorene. For instance, mechanical exfoliation yields high-quality, atomically thin flakes ideal for fundamental studies, while LPE offers a more scalable route for producing phosphorene for applications that can tolerate some size and thickness variations. CVD and MBE are well-suited for situations requiring precise control over layer thickness and uniformity, particularly in nanoelectronics device fabrication.

Top-down techniques separate the layers of bulk BP by breaking the weak van der Waals forces between them, resulting in single-layer or few-layer nanosheets. Bottom-up techniques synthesise phosphorene directly from molecular precursors [79]. Common top-down methods

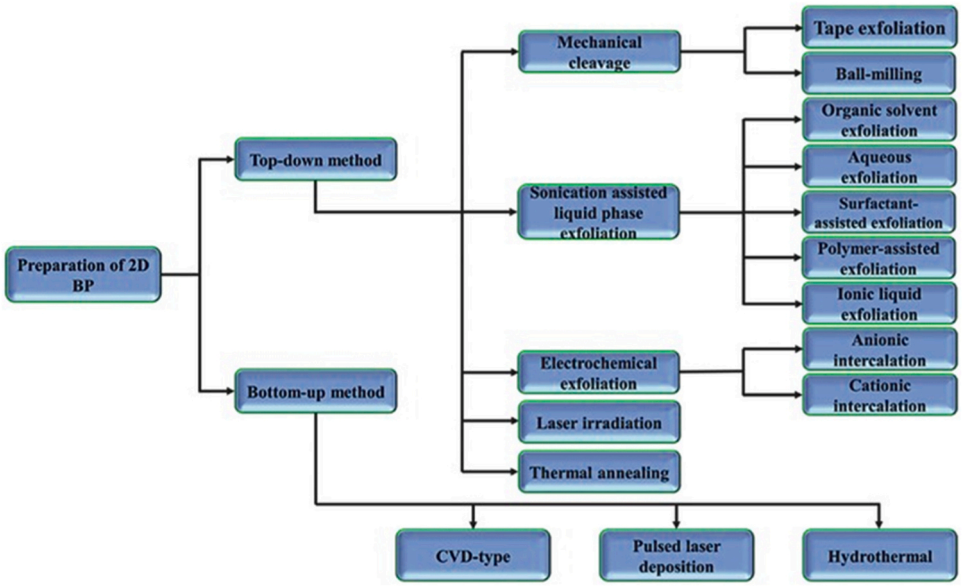

Fig. 4. Overview of Preparation Strategies for Fabricating Two-Dimensional (2D) Few-Layer Black Phosphorus (BP) and Phosphorene [79].

include mechanical exfoliation (the "Scotch tape" method), which was first used for isolating graphene. It can produce high-quality BP nanosheets, but it is not scalable and requires specialised equipment [81,82]. Liquid-phase exfoliation (LPE) disperses bulk BP in solvents such as N-methyl-2-pyrrolidone (NMP) or dimethylformamide (DMF) to produce phosphorene nanosheets. LPE can generate larger quantities without expensive equipment and can be combined with techniques such as ultrasonication and electrochemical processes [83]. However, LPE can be challenging to achieve uniform size and thickness control. Other synthesis methods offer specific benefits. Solvothermal methods enable low-cost production of BP nanoparticles and nanocrystals with tuneable properties [84]. Hydrothermal synthesis produces BP in various morphologies by heating precursors in water under high pressure, but it is time- and energy-consuming. Pulsed laser deposition (PLD) produces high-quality, uniform BP films with precise control over thickness and composition, but it requires specialised equipment and is not suitable for large-scale production [85–88]. Among these methods, mechanical exfoliation, liquid exfoliation, and plasma etching are widely used for BP fabrication because they rely on breaking the weak van der Waals forces between layers [89–92]. Several methods have been devised to improve the synthesis of BP nanosheets. Guo et al. [93] were the first to isolate monolayer BP through a combination of mechanical exfoliation and plasma etching. To increase yield, methods assisted by metal have been introduced [94]. To enhance the effectiveness of mechanical exfoliation, dry transfer techniques using thermal-release tape or PDMS stamps have been developed. However, scalability for large-scale device production is still a challenge [95–97]. Liquid-phase exfoliation (LPE) of ultra-thin BP can be achieved using various solvents in combination with ultrasonication or electrochemical processes [98,99]. The choice of solvent significantly affects yield, with the surface tension matching the surface energy of the bulk material being vital. NMP-assisted exfoliation enhances stability by introducing hydroxyl groups onto the BP surface. The size of BP can be controlled by adjusting the power and duration of sonication [100]. While LPE often uses environmentally harmful solvents, emerging "green" methods use ionic liquids (ILs). These promote dispersion interactions through weakly coordinating ions and group grafting [101,102]. Electrochemical exfoliation is a promising method for obtaining high-quality BP. This approach includes specific techniques such as cationic intercalation and anodic oxidation [103,104]. Anodic oxidation with aqueous electrolytes has enabled the isolation of BP down to a few atomic layers. However, while cation insertion facilitates damage-free phosphorene synthesis, these cations can be partially oxidised via anion insertion, potentially affecting BP and phosphorene characteristics. This can be mitigated by water rinsing [105,106]. Chemical vapour deposition (CVD) is an effective technique for synthesising phosphorene. It allows for scalable production with control over layer characteristics. Furthermore, CVD enables precise doping, integration with other materials, and the growth of high-quality BP films, making it suitable for large-scale manufacturing. However, it requires specialised expertise, expensive equipment, and consumes time and energy [107]. Molecular beam epitaxy (MBE), conducted in an ultra-high vacuum environment, allows for the epitaxial growth of phosphorene on selected substrates. Precise control of phosphorous evaporation via beams produces phosphorene with exceptional crystallinity and flexible layering. However, its low yield and high cost of instrumentation are limiting factors [108]. Additional hybrid methods include pulsed laser deposition (PLD) and electrochemical exfoliation. PLD deposits-controlled phosphorene films by ablating BP targets with high-energy laser pulses. However, this method offers only moderate tunability and layer thickness control [109]. Electrochemical exfoliation uses electric current and potential within an electrolytic solution to exfoliate bulk BP, with adjustable parameters influencing the process. However, the potential introduction of defective phosphorene and impurities are concerns [110]. Direct chemical synthesis of few-layer BP faces challenges associated with the air instability of BP, leading to underexplored pathways compared with top-down methods [77]. This process comprises three stages: nucleation, island expansion, and film formation [111]. Techniques such as PLD and in-situ CVD have shown success in synthesising BP [112]. The choice of substrate is crucial, with flexible and single-crystal metal substrates reducing defects and improving BP quality [113,114]. Optimisation of pressure and temperature control is key to enhancing large-scale production and elucidating the underlying growth mechanisms. Direct synthesis using red phosphorus (RP) thin films as precursors promises scalability [115,116]. Surface passivation is a crucial step in enhancing the usability of BP. Techniques that use organic solvents or 2D materials for encapsulation can extend its stability and broaden its application potential [112,115,117]. For real-world applications, it's essential to produce phosphorene on a large scale and of high quality. Given its vulnerability to oxidation and hydrolysis, it's important to carefully manage the ambient conditions during production. Maintaining consistency in thickness and lateral dimensions is key to ensuring reproducibility and reliable device performance [118]. The properties of phosphorene can be customised through surface

modifications. Techniques such as chemical functionalisation, metal doping, and the creation of 2D hetero composites can alter its electronic structure, reactivity, and stability [119–121]. Table 3 offers a comparison of various phosphorene synthesis techniques, highlighting the advantages and drawbacks of each.

2.3. Black phosphorus and phosphorene: structure, properties, and characterisation

Black phosphorus (BP) and phosphorene are structurally related forms of phosphorus, both characterised by a layered arrangement. However, the number of layers and the strength of interlayer bonding significantly impact their properties. BP consists of multiple covalently bonded phosphorus atoms stacked in a puckered honeycomb lattice, held together by weak van der Waals forces [44,133]. This layered structure, confirmed by X-ray diffraction (XRD) analysis [134,135], grants BP its anisotropic characteristics – properties that vary depending on direction. In contrast, phosphorene represents a single or few-layered variant, where individual layers are held together by even weaker van der Waals interactions [136]. This difference translates to a more flexible nature for phosphorene compared to the rigid, layered structure of BP [44,133]. The variations in structure between BP and phosphorene lead to distinct properties that make them attractive for various applications. BP exhibits a wider bandgap than phosphorene, making it suitable for high on/off ratio devices in electronics [137,138]. Additionally, BP's anisotropic electronic characteristics offer unique advantages for device design. However, BP can be susceptible to instability under certain conditions [138]. Conversely, phosphorene boasts a tuneable bandgap that can be adjusted based on the number of layers, offering greater flexibility for optoelectronic applications [136]. The non-uniform electron distribution within phosphorene's structure, influenced by the number of layers, also contributes to its unique properties. Notably, few-layered phosphorene exhibits enhanced stability compared to its monolayer counterpart [138]. X-ray diffraction (XRD) serves as a crucial tool for investigating the atomic arrangement within BP and phosphorene. BP's characteristic XRD pattern features prominent peaks corresponding to specific crystal planes, such as (020), (040), and (060), which reveal information about interlayer spacing and crystal structure [134,135]. Additionally, peaks associated with (002) and (004) planes confirm BP's layered nature. These peaks correspond to specific "d-spacing" values, providing detailed structural information. Conversely, phosphorene exhibits a distinct XRD pattern indicative of its orthorhombic unit cell with well-defined dimensions. The unique puckered honeycomb lattice structure of phosphorene, characterised by sp^3 hybridised phosphorus atoms, imparts a partially metallic character to the material. This structure also leads to remarkable anisotropy in various properties of phosphorene, including electrical conductivity, thermal conductivity, vibrational behaviour, and mechanical characteristics [139–141]. This anisotropy arises due to the presence of two primary directions within the material: the armchair and zigzag directions. Studies have shown that electrical conductivity is lower in the armchair direction compared to the zigzag direction [142,143]. Both BP and phosphorene exhibit the ability to undergo reversible phase transformations when subjected to high pressure or temperature conditions [142]. These transformations lead to the formation of new phases with distinct crystal structures, such as orthorhombic, rhombohedral, and simple cubic [144–146]. Interestingly, some of these high-pressure phases exhibit superconductivity, a phenomenon that has garnered significant research interest in phosphorus allotropes [61,147,148]. X-ray diffraction (XRD) and polarisation-resolved Raman scattering (PRRS) serve as crucial techniques for investigating the structural and anisotropic properties of BP and phosphorene. As discussed earlier, XRD analysis provides valuable information about the crystal structure of a material. In the case of BP, the characteristic XRD pattern with specific peaks (Fig. 5a) allows researchers to determine its lattice parameters [134]. This information is essential for understanding the arrangement of atoms within the BP crystal structure. Polarisation-Resolved Raman Scattering (PRRS) offers a powerful tool for exploring the anisotropic properties of BP (Fig. 5b) [149,150]. Raman spectroscopy itself relies on scattered light to identify a material's vibrational modes (phonons), which provide insights into its structure. PRRS takes this a step further by controlling the polarisation of both the incident and scattered light. This enables researchers to observe that BP's vibrational modes vary along different crystallographic directions. By selectively activating or strengthening specific modes based on light polarisation, PRRS provides detailed information about the material's directional characteristics. This technique is particularly valuable for detecting defects or strain within the BP lattice [151–153]. Notably, PRRS can also be used to study the high-pressure phase transitions of BP, which hold promise for superconductivity research [140,141]. Beyond BP, phosphorene is attracting significant interest for its potential applications in optoelectronics. This is attributed to its unique combination of properties, including a planar structure, a direct bandgap, strong light-matter interaction, and high carrier mobility [154]. Both BP and phosphorene exhibit a fascinating characteristic – their bandgap and other properties can be tuned based on the number of layers they contain [155,156]. This tunability makes them highly materials for various device applications. Notably, the unique band structure of single-layer BP, also known as

Table 3
Comparison of Different Synthesis Methods for Phosphorene.

Synthesis Technique	Condition and Remarks	References
Liquid-Phase Exfoliation (LPE)	Simple, scalable method with challenges in controlling thickness and quality. Solvent: NMP. Sonication for exfoliation. Room temperature. Concentration of black phosphorus in solvent. Challenges: Thickness, Quality, Stability.	[122]
Chemical Vapor Deposition (CVD)	Scalable method with precise control. Requires expensive equipment and expertise. Deposition using PH_3, H_2, or Ar. Temperature: 500–1000°C. Pressure control. Substrate choice influences nucleation. Precise control over thickness, orientation.	[123]
Electrochemical Synthesis	Low-cost, scalable method with precise control. Applicable to various substrates. Voltage influences overpotential, material expansion, and electrolyte color. Higher Voltage: Accelerates reactions, enhances exfoliation, risks degradation. Lower Voltage: Safer, slower, longer exfoliation.	[52, 123–125]
Mechanical Exfoliation	Simple, effective method with challenges in thickness control.	[54]
Solvothermal Synthesis	Yields phosphorene via mechanical or liquid-phase exfoliation.	[53]
Laser Ablation	Produces high-quality phosphorene. Requires expensive equipment.	[53–55]
Plasma-assisted Mechanical Exfoliation	Uses plasma treatment to enhance quality and yield.	[53,54,126]
Plasma-liquid Exfoliation	Efficient production of 2D materials with minimal oxidation.	[127]
Direct solvothermal process	Produces few-layer BP nanosheets. Flake thickness decreases with temperature.	[128]
Growth of 2D phosphorene	Forms nanoclusters and single atoms on Cu (111) surfaces. Weak interactions favor extended layers.	[124,129]
Molecular beam epitaxy (MBE) growth	Produces few-layer BP quantum dots. Material degradation observed.	[130]
Exfoliation in isopropanol-water cosolvents	Yields monolayers and bilayers under specific conditions. Water presence affects stability.	[131]
Impact of water on phosphorene stability	Small water amounts enhance synthesis quality. Optimal phosphorus/water ratio maximizes quality.	[132]

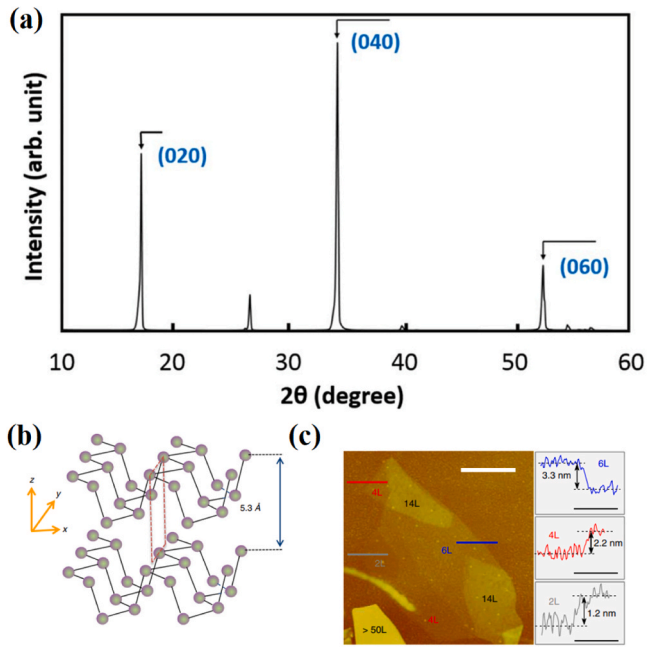

Fig. 5. (a) The XRD pattern of black phosphorus crystals reveals distinct peaks that correspond to the (020), (040), (060) crystal planes [134], b) The figure displays the layered crystal structure of black phosphorus, with two adjacent puckered sheets consisting of linked phosphorus atoms. The layer-to-layer spacing in BP is approximately 5.3 Å, (c) AFM image on the left, indicating estimated black phosphorus layer numbers, with a 2 mm scale bar; on the right, line scans reveal layer numbers (2−450) based on thickness, with a 1 mm scale bar [158].

phosphorene, distinguishes it from its multi-layer and bulk counterparts, contributing to its remarkable potential [157]. However, for real-world device integration, surface modifications are often necessary to enhance the stability of these materials [136]. Atomic Force Microscopy (AFM) provides a complementary technique for confirming the layered structure of BP, as illustrated in Fig. 5c [150]. This high-resolution imaging technique allows researchers to visualise individual BP flakes and directly measure their thickness. The image in Fig. 5c shows flakes with varying layer counts, and the accompanying line scans quantify these variations, ranging from a few layers to hundreds. This information is crucial for understanding the impact of layer number on the properties of BP and phosphorene.

While various methods can produce few-layered BP, including mechanical cleavage, liquid exfoliation, and chemical vapor deposition (CVD), phosphorene is typically obtained through the exfoliation of bulk BP crystals [159,160]. A significant challenge lies in scaling up BP production while maintaining its quality, as it is susceptible to oxidation and degradation. Cathodic exfoliation in water has emerged as a promising strategy to mitigate the degradation of few-layered BP flakes during the exfoliation process [161]. For phosphorene, alternative strategies beyond exfoliation are being explored to increase yield and expand its potential applications. Electrosynthesis and covalent macromolecular attachment are two such techniques gaining traction [45,162]. Fig. 6 provides representations of these approaches. Scanning Electron Microscopy (SEM) plays a crucial role in analysing the morphology of BP crystals after exfoliation under different processing conditions (Fig. 6a-d) [150,163]. Annular Dark-Field Scanning Transmission Electron Microscopy (ADF-STEM) offers high-resolution imaging capabilities, revealing the characteristic layered 2D structure of BP at the flake edges and confirming its [100] crystallographic orientation [161]. These imaging techniques, combined with the understanding that aqueous exfoliation necessitates higher voltages and the protective role of cationic surfactants like CTA+, provide valuable insights for optimising scalable production strategies. Beyond synthesis, various strategies are employed for the functionalisation of BP, including electrosynthesis, covalent macromolecular attachment, and chemical modification [45,162]. Fig. 6e and f illustrate this concept, with cross-sectional analysis by ADF-STEM revealing the alignment of layers (in the [100] direction) within a BP flake. This high-resolution imaging is essential for detecting foreign atom doping, a powerful technique for tailoring BP's properties. Given that the bandgap of BP varies significantly with layer count, it is essential to conduct both theoretical and experimental investigations of its bandgap behaviour across different thicknesses [164]. Characterisation techniques like ADF-STEM imaging and polarisation-resolved Raman spectroscopy play a vital role in this endeavour. These techniques offer insights into BP's layered structure and enable the detection of foreign atom doping, a powerful method for controlling BP's electronic and optical behaviour [165].

The layered crystal orientation of black phosphorus (BP) is a critical factor when interpreting results obtained from polarisation-resolved Raman scattering (PRRS) [150]. Raman spectroscopy, a powerful characterisation tool, utilises scattered light to identify the vibrational modes (phonons) of a material, which provide insights into its crystal structure. PRRS takes this analysis a step further by controlling the polarisation of both the incident and scattered light. This enables researchers to probe the anisotropic nature of BP, where its properties vary depending on direction. The Raman spectra of BP exhibit distinct signatures that reveal its orthorhombic crystal structure. Characteristic A_2g, B_2g, and A_1g modes are typically observed near 470 cm^{-1}, 440 cm^{-1}, and 365 cm^{-1}, respectively. In contrast, phosphorene possesses unique PRRS signatures with characteristic peaks around 363 cm^{-1}, 480 cm^{-1}, and 243 cm^{-1}, corresponding to its A_1g, B_2g, and A_2g modes, respectively [163]. When light interacts with these materials, the intensity of these Raman modes varies depending on the polarisation of the light relative to the crystallographic axes of BP or phosphorene. This variation in intensity arises from the anisotropic nature of these materials. Phosphorene's distinctive structure, characterised by a direct bandgap and high carrier mobility, contributes to its strong light-matter interaction. This property makes phosphorene a promising candidate for various optoelectronic applications. Additionally, techniques like doping and strain engineering can further manipulate these properties, enabling the development of materials with tailored functionalities [166]. PRRS offers a particularly valuable tool for determining the crystal orientation of small BP flakes, which can be challenging to characterise using other techniques. As illustrated in Fig. 7, PRRS analysis of a layered BP thin film highlights the anisotropy of BP's vibrational modes [150]. By controlling the polarisation of the incident and scattered light, PRRS allows researchers to identify the distinct crystal axes and orientation of individual BP flakes. Furthermore, PRRS can be employed to study the effects of strain, doping, and defects within the BP lattice [167]. This makes PRRS a comprehensive tool for characterising not only BP but also other 2D materials with anisotropic properties.

Black phosphorus (BP) and phosphorene exhibit unique properties that make them attractive candidates for various applications beyond conventional electronics. One particularly intriguing phenomenon is superconductivity, a state where a material exhibits perfect electrical conductivity with zero resistance. This phenomenon holds immense promise for applications in power transmission, energy storage, and high-speed electronics [168,169]. Notably, both BP and phosphorene have been shown to exhibit superconductivity under specific conditions, such as high pressure, doping with foreign atoms, or intercalation (insertion of guest atoms between layers) [166]. The superconducting properties of BP and phosphorene are intricately linked to their crystal structures. Techniques like X-ray diffraction (XRD) and polarisation-resolved Raman scattering (PRRS) play a crucial role in elucidating these structures [80]. XRD analysis provides insights into the arrangement of atoms within the crystal lattice, while PRRS allows researchers to probe the material's anisotropic properties (properties that

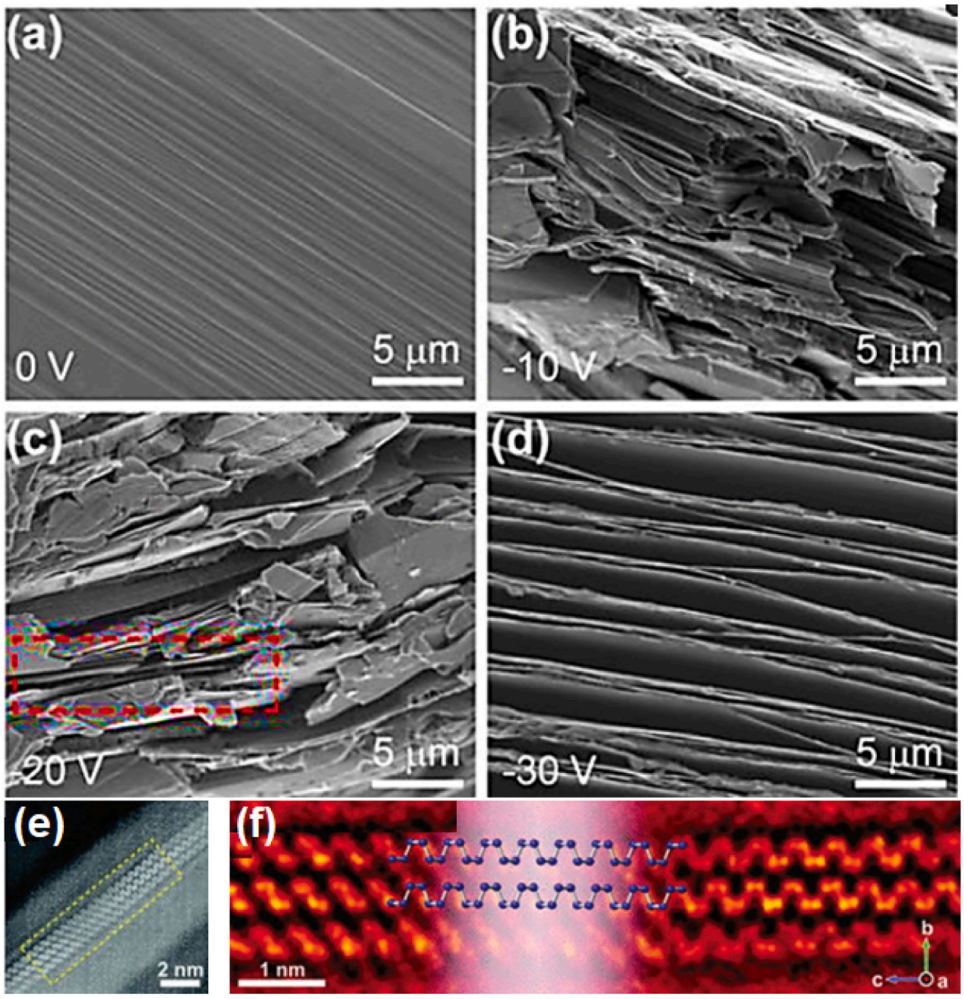

Fig. 6. (a-d) Scanning electron microscopy (SEM) images for bulk BP crystals after being subjected to different voltages at 50 °C. Specifically, the images correspond to: (a) 0 V; (b) −10 V; (c) −20 V; and (d) −30 V[161], (e-f) Low- and high-magnification ADF-STEM images of layered 2D BP captured at the edge of a BP flake oriented along the [100] crystallographic direction [164].

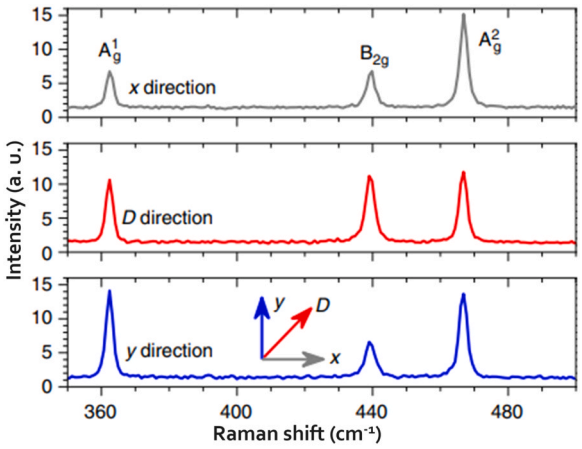

Fig. 7. Polarisation-resolved Raman scattering on a layered BP thin film using a 532-nm linearly polarised laser in the z direction, consistently observing A_2g, B_2g, and A_1g modes with significant intensity variations based on polarisation direction, proving beneficial in identifying crystalline orientation, particularly for small flakes, due to the small laser spot size (B1–2 mm) [163].

vary depending on direction). By understanding the relationship between crystal structure and superconductivity in BP and phosphorene, researchers can explore novel methods to manipulate and enhance their superconducting performance for future technologies. Table 4 summarises the common characterisation techniques employed for BP and phosphorene, along with their functionalities.

2.3.1. *Black phosphorus and phosphorene: structure-driven properties*

Black phosphorus (BP) and its single-layer counterpart, phosphorene, have garnered significant research interest due to their exceptional structure-property relationships [119,178]. BP possesses a layered structure, where individual phosphorene sheets are stacked together. These phosphorene sheets, consisting of a few phosphorus atoms arranged in a puckered honeycomb lattice, result from sp^3 hybridisation of phosphorus orbitals [3]. Weak van der Waals forces bind these layers within BP, enabling their exfoliation into few-layered or single-layer (phosphorene) structures [119]. The remarkable properties of BP and phosphorene make them promising candidates for diverse applications. For instance, BP boasts a theoretical specific capacity of 2596 mAh/g, exceeding that of graphite by nearly sevenfold, positioning it as a potential game-changer in energy storage applications [178]. Phosphorene, on the other hand, is sought after for its unique electrical, optical, physical, and electrochemical properties. These include a tuneable bandgap, high conductivity, and exceptional carrier mobility – traits that pave the way for advanced sensing materials in healthcare,

Table 4
Characterisation Techniques for Black Phosphorus and Phosphorene.

Characterisation Technique	Purpose and Insights Gained	References
Optical Microscopy	Assess sample quality and morphology, determine layer thickness and number, identify flake size and distribution, detect defects and impurities in black phosphorus and phosphorene.	[143,151]
Atomic Force Microscopy	Measure surface topography and thickness, provide precise measurements of surface roughness and topography, determine layer thickness and heights in black phosphorus and phosphorene.	[22,169]
Scanning Electron Microscopy	High-resolution imaging of surface morphology, edge structure, defects, determine flake size, shape, and uniformity in black phosphorus and phosphorene.	[139,168]
Transmission Electron Microscopy	Analyse atomic-level structure and crystallinity, provide atomic-scale resolution of crystal structure and defects, determine lattice parameters in black phosphorus and phosphorene.	[168,169]
Raman Spectroscopy	Study vibrational properties and layer identification, identify layer thickness and stacking order, analyse phonon modes, lattice vibrations, strain-induced changes in black phosphorus and phosphorene.	[153,170]
X-ray Diffraction	Determine crystalline structure and phase, identify crystal structure, phase transitions, orientation, measure lattice parameters in black phosphorus and phosphorene.	[27,171, 172]
X-ray Photoelectron Spectroscopy	Analyse chemical composition and oxidation states, determine elemental composition, oxidation states, investigate surface chemistry, functional groups in black phosphorus and phosphorene.	[28,172, 173]
Photoluminescence Spectroscopy	Investigate electronic band structure and excitonic behaviour, study bandgap properties, electronic structure, defects, impurities, exciton dynamics, exciton emission in black phosphorus and phosphorene.	[174–176]
Electrical Transport Measurements	Study carrier mobility and conductivity, measure charge carrier mobility, conductivity, resistivity, assess electronic properties, device performance in black phosphorus and phosphorene.	[176,177]

batteries, transistors, and photovoltaics. Notably, phosphorene's high conductivity, carrier mobility, tensile strength, and biocompatibility make it particularly attractive for both electrical and biomedical applications [119]. BP and phosphorene are particularly well-suited for applications in electronics and optoelectronics, where efficient heat dissipation, high carrier mobility, and a tuneable bandgap are highly desirable [179]. Phosphorene, in particular, stands out due to its direct bandgap and flexible hexagonal lattice, contributing to both its robust mechanical properties and efficient light absorption and emission [180, 181]. This unique combination makes phosphorene a valuable material for photodetectors, solar cells, LEDs, transistors, and energy storage devices. It offers potential advantages such as faster switching speeds, lower energy consumption, a wide absorption range, and an adjustable bandgap [179,181]. Despite their immense potential, BP and phosphorene research still face challenges and exciting opportunities. Key areas for exploration include developing cost-effective and scalable synthesis methods. A deeper understanding and control over the growth mechanisms and properties of phosphorene are crucial. Additionally, research efforts are focused on enhancing the stability and degradation resistance of phosphorene, along with efficient methods for its transfer and integration into device structures. Finally, unravelling the factors influencing bandgap tuning in phosphorene remains an important research direction [180]. BP exhibits an indirect bandgap in its bulk form, limiting its light-matter interaction and hindering its performance in optoelectronic applications. In contrast, phosphorene boasts a coveted direct bandgap, making it a superior choice for optoelectronic devices. Furthermore, BP exhibits strong in-plane anisotropy, meaning its properties vary depending on the direction of measurement. Phosphorene exhibits less anisotropy, offering greater material uniformity. While both materials possess good carrier mobility, phosphorene outperforms BP in this aspect, making it more favourable for high-performance electronics. Their low effective mass translates to rapid charge transport, a desirable trait for various electronic and optoelectronic devices [182]. The bandgap of BP is remarkably dependent on the number of layers due to quantum confinement and electronic structure changes. As the number of layers decreases (moving from bulk BP to few-layer BP and ultimately to single-layer phosphorene), electrons and holes become confined within a smaller space. This confinement alters the energy levels and increases the bandgap due to stronger Coulomb interactions (reduced screening compared to bulk BP). This shift from a wider bandgap in few-layer BP to a narrower bandgap in bulk BP makes it strategically useful for specific electronics and optoelectronics applications [167]. Phosphorene's electronic properties are remarkably sensitive to external influences such as electric fields and doping. A distinct feature of phosphorene is its bilayer bandgap, which can vary between 0.78 eV and 1.04 eV. This variation is attributed to the interlayer distance (ranging from 3.21 Å to 3.73 Å) and the specific stacking order of the phosphorene layers [183]. A well-established approach involves manipulating the number of layers. As the dimensionality transitions from bulk to monolayer phosphorene, the bandgap widens significantly, increasing from around 0.3 eV to approximately 2 eV. Recent research efforts have placed significant emphasis on using functionalisation and doping to achieve precise control over the bandgap and other properties of phosphorene. For instance, studies have shown that oxygen atoms readily adsorb onto the reactive edges of phosphorene, enhancing its stability. Covalent diazonium functionalisation offers a similar advantage, effectively suppressing chemical degradation and significantly improving the overall stability of phosphorene. Electronic properties can also be manipulated through targeted doping strategies. The addition of Cu adatoms or chemical doping with benzyl viologen have been demonstrated as effective methods for n-type doping, enabling researchers to achieve n-type conductivity in phosphorene. Interestingly, even dopants like oxygen, sulphur, or selenium, which are not inherently magnetic, can induce magnetism in phosphorene upon incorporation. This phenomenon is attributed to the bonding configuration, where these dopant atoms bond with only two phosphorus atoms, leaving an unpaired electron. Similar magnetic effects have been predicted for blue phosphorene using theoretical calculations. Fig. 4 summarises the diverse strategies reported in the literature for tailoring the bandgap of phosphorene. Notably, the figure highlights the significant increase in bandgap achieved by reducing dimensionality from bulk to monolayer phosphorene, as shown in Fig. 8 [121].

Interlayer forces and quantum confinement play a crucial role in this phenomenon. AA-stacking, where phosphorus atoms are vertically aligned, leads to stronger interlayer coupling and consequently, a smaller bandgap compared to AB-stacking (atoms horizontally offset). The weaker interaction in AB-stacking results in a wider bandgap. Quantum confinement also contributes, although to a lesser extent. AA-stacking's slightly larger interlayer distance translates to weaker confinement, further reducing the bandgap [184–186]. Layer count and van der Waals forces also influence phosphorene's electronic properties. These factors lead to a combination of quantum confinement, interlayer interaction, and G-point effects within the Brillouin zone. As the number of layers decreases (stronger quantum confinement), charge carriers

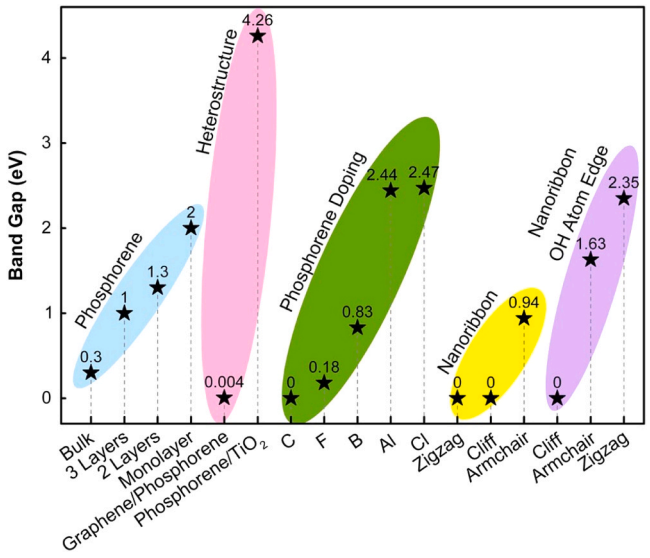

Fig. 8. Energy band gap engineering of black phosphorus, and engineered phosphorene[121].

become restricted within the two-dimensional plane. This alters the energy levels and widens the bandgap. The weak van der Waals bonds allow the layers to slide, affecting the charge distribution and band structure. These interactions further influence the G-points in the Brillouin zone, which are critical determinants of phosphorene's electronic behaviour. This combined effect leads to a wider bandgap near the Fermi level and at the G-points, making phosphorene suitable for high-performance transistors and optoelectronic devices where controlling carrier concentration while minimising absorption/emission transparency is crucial. Notably, the valence band maximum (VBM) and conduction band minimum (CBM) of phosphorene are situated at the G-points, high-symmetry positions in the Brillouin zone. The bandgap value in phosphorene can be effectively tuned using various strategies. These include changing the number of layers, applying strain, or utilising an electric field [184]. Additionally, phosphorene's anisotropic optical response reflects its sensitivity to variations such as increased magnetic fields [187]. Few-layer BP exhibits high electron mobility, a desirable trait for electronic applications. Interestingly, it also displays anisotropic, hole-dominated transport, offering additional possibilities for device design [149]. A significant challenge for both BP and phosphorene is their reactivity and vulnerability to environmental factors. Their inherent reactivity can lead to the formation of composites or chemisorption. BP, in particular, degrades readily when exposed to H_2O and O_2 [188,189]. Phosphorene, by virtue of being the single-layer form of BP, offers certain advantages over its bulk counterpart. Its lower surface area and reduced exposure to the environment make it less susceptible to oxidation and degradation. Additionally, phosphorene possesses isotropic electronic properties and a tuneable semiconducting bandgap, both of which are influenced by the number of layers. These features make phosphorene an attractive material for optoelectronic and electronic applications that demand high charge carrier mobility and rapid relaxation dynamics [25,190]. However, despite these advantages, phosphorene remains susceptible to environmental instability [150]. BP, on the other hand, exhibits remarkable optical and superconducting properties that are intricately linked to its crystal structure and pressure. When subjected to high pressure, BP undergoes phase transitions, resulting in diverse structures like A17, A7, and pseudo-simple-cubic (p-Sc). These structures exhibit distinct interlayer bonding characteristics and bandgap values, ultimately affecting the electronic and optical behaviour of BP [61,191]. Additional studies have shed light on BP's fascinating pressure-induced superconducting response. These studies employ synchrotron X-ray diffraction to analyse the structural changes under pressure, utilising various pressure-transmitting media such as helium, hydrogen, nitrogen, and Daphne Oil 7474. Notably, the findings reveal that irrespective of the chosen medium, BP undergoes transitions through A17, A7, and pseudo-simple-cubic (p-Sc) structures above 10.5 GPa. These structures can be categorised as follows: A17 and A7 possess layered structures with weak interlayer interactions, while p-Sc exhibits a distorted-cubic structure with a combination of s and p orbitals influencing bonding[191]. Interestingly, BP also demonstrates superconductivity above a critical pressure, which crucially depends on the specific pressure-transmitting medium used. This observation underscores the influence of the surrounding environment on BP's superconducting behaviour. Understanding the structural evolution of BP under pressure is essential for elucidating its unique properties and potential applications. Synchrotron X-ray diffraction, along with other characterisation techniques, plays a crucial role in revealing the phase transitions that BP undergoes during compression, as demonstrated in various studies [61,191]. Phosphorene (single-layer BP) exhibits high chemical reactivity due to the lone electron pairs associated with specific phosphorus atoms in its puckered honeycomb lattice. These reactive sites readily participate in reactions with various compounds and nanoparticles, paving the way for the design of advanced 2D BP-based systems with tailored properties. Examples of such interactions include bonding with organic groups, metal, or metal oxide nanoparticles, other inorganic 2D materials, or polymers[192,193]. These interactions can significantly modify various properties of phosphorene, including its bandgap, charge transfer efficiency, stability, magnetism, photocatalytic activity, optoelectronic behaviour, mechanical strength, thermal properties, electrical conductivity, and biodegradability. Decorating phosphorene with metal or metal oxide nanoparticles introduces exciting new functionalities. For instance, gold nanoparticles have been shown to enhance phosphorene's photocatalytic water splitting capabilities, while iron oxide nanoparticles can impart magnetic properties, making it a promising candidate for spintronic applications. A critical challenge for phosphorene is its susceptibility to degradation by oxygen, water, and light, which can significantly impair its performance. To address this issue, researchers have developed various strategies, including thin metal oxide or polymer coatings (e.g., Al_2O_3, ZnO, PVA). These passivation layers not only enhance the stability of phosphorene but also offer the potential for bandgap modulation [78,194]. Furthermore, the weak interlayer bonding in phosphorene allows for the formation of heterostructures with other inorganic 2D materials such as graphene, MoS_2, WS_2, and transition metal dichalcogenides (TMDCs). This approach provides precise control over band alignment, improved carrier mobility, and ultimately, enhanced optoelectronic performance. The integration of phosphorene into polymers such as PVA, PEG, and PLA leads to the development of composites with superior mechanical strength, thermal stability, electrical conductivity, and biodegradability [195,196]. Despite the promising advancements in functionalising phosphorene, a significant challenge remains: protecting BP and phosphorene from degradation caused by oxygen, water, and light. While various strategies like coating, passivation, encapsulation, and doping have been explored to improve stability, they may introduce drawbacks such as increased processing complexity, unintended changes in behaviour, or the introduction of defects and impurities [196,197]. Phosphorene's unique structure leads to a remarkable in-plane anisotropy, where properties differ significantly between the armchair (AM) and zigzag (ZZ) directions. This is evident in the effective mass of charge carriers, with holes exhibiting up to eight times larger mass along ZZ compared to AM. The disparity extends to phonon dispersion and translates to a strong anisotropy in shear modulus and thermal transport. Beyond these examples, anisotropy influences electron-photon and electron-phonon interactions depending on thickness and spectral characteristics. Notably, theoretical predictions suggest an anisotropic magnetic nature and the possibility of a dissipative quantum Hall effect for ZZ edges. Strain can be used to manipulate anisotropy and tailor properties. As shown in Fig. 9(a, b), the effective mass of electrons and

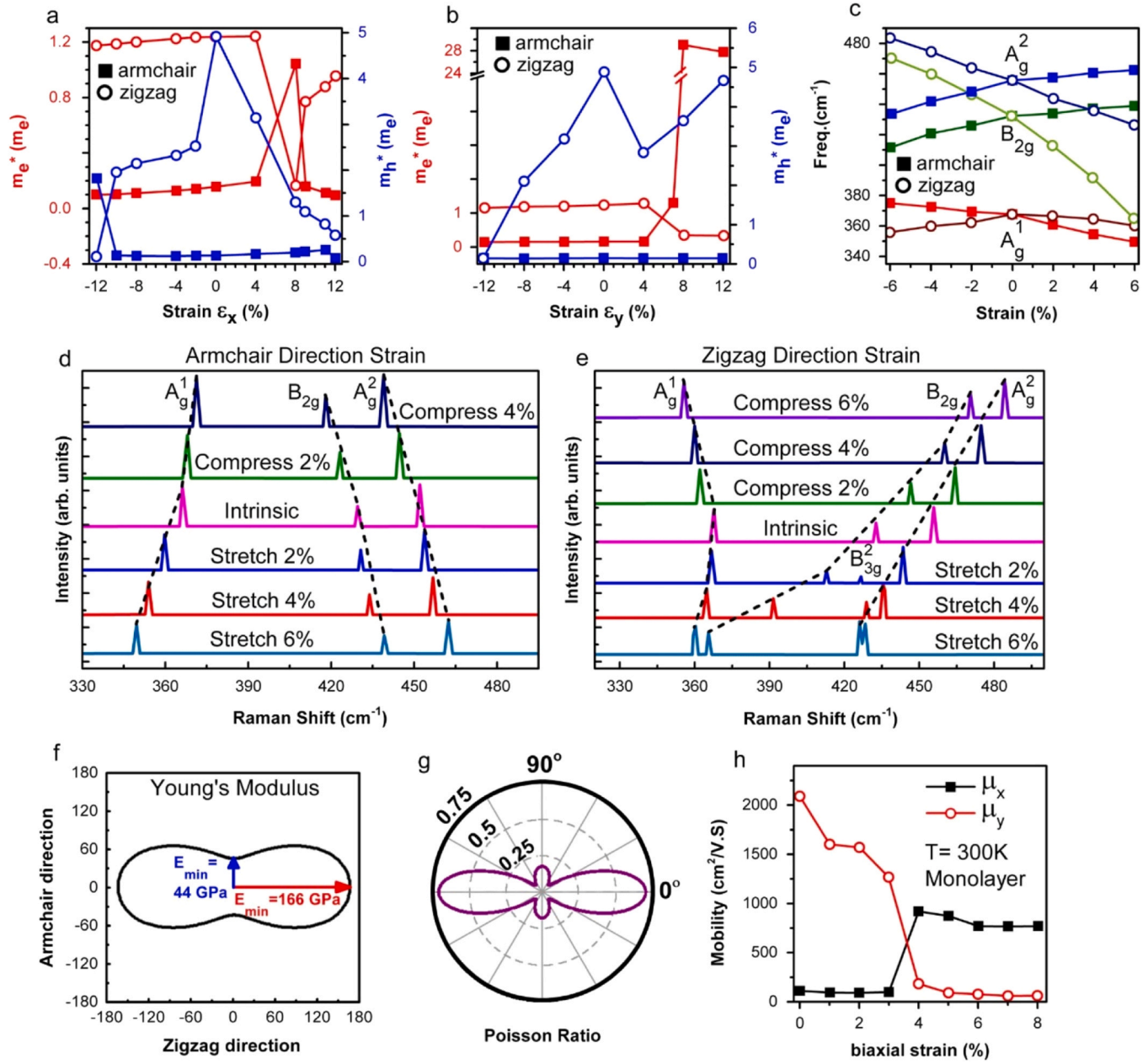

Fig. 9. (a, b) Effective masses of the electron and hole under uniaxial strain "ε" in both the zigzag "x" and armchair "y" directions, respectively. (c) Frequency of Raman modes of phosphorene (Ag_1, B_2g, and Ag_2) as a function of uniaxial strain along zigzag and armchair directions. (d, e) Raman spectra of phosphorene as a function of uniaxial strain along zigzag and armchair directions, respectively. (f, g) Direction dependence of Young's modulus and Poisson's ratio of phosphorene. (h) Electron mobility of phosphorene along zigzag (μx) and armchair (μy) directions as a function of biaxial strain at room temperature [121].

holes depends on strain direction, highlighting the interplay between strain and charge transport. Raman spectroscopy (Fig. 9c-e) provides a tool to identify strain direction and magnitude based on the shift and pattern changes in Raman peaks under strain. Phosphorene's mechanical properties also exhibit anisotropy. The Young's modulus (Fig. 9f) varies significantly between ZZ and AM directions due to the material's puckered structure. Similarly, the Poisson's ratio displays anisotropy (Fig. 9g). Remarkably, even the charge transport characteristics are affected (Fig. 9h), with electron mobility along ZZ exceeding that along AM under specific biaxial strain, offering opportunities for strain-engineered transport properties [121].

3. Black phosphorus and phosphorene nanocomposites for enhanced performance through synergistic design

Black phosphorus (BP) and its single-layer counterpart, phosphorene, possess remarkable properties like anisotropic characteristics, high carrier mobility, and a tuneable bandgap [198]. These exceptional attributes make them attractive candidates for diverse applications in electronics, optoelectronics, energy storage, and biomedicine [199–201]. However, their susceptibility to oxidation and degradation under ambient conditions hinders their long-term stability and integration into practical devices. A promising approach to address the stability limitations of BP and phosphorene involves integrating them with nanoparticles to form nanocomposites within a polymer matrix. These nanocomposites offer enhanced properties and performance compared to the individual components [202–204]. Several synthesis

methods have been established for the fabrication of BP and phosphorene nanocomposites, including one-pot synthesis, in-situ polymerisation, solvent-mediated exfoliation, and mechanical exfoliation. Studies have demonstrated the effectiveness of BP-based nanocomposites in significantly improving the fire resistance of polymers. For instance, the exceptional refractory performance observed in waterborne polyurethane composites is attributed to the synergistic effect between BP and boron nitride (BN) in both the gas and condensed phases [4]. However, incorporating BP alone can negatively impact the mechanical properties of the polymer matrix. Researchers have successfully addressed the challenge of compromised mechanical performance by incorporating graphene [182] into BP/polymer nanocomposites. The addition of phosphorene/graphene not only significantly improves the thermal stability of waterborne polyurethanes (WPUs) but also demonstrably enhances their Young's modulus, indicating improved mechanical performance [205]. Functionalisation techniques offer a strategic approach to enhancing the performance of BP nanocomposites. Studies have explored various types of polymers for this purpose. Polyphosphazene (PZN), for instance, demonstrably improves BP's stability through covalent bonding or electrostatic interactions [198]. Beyond PZN, researchers can strategically select polymers like polyphosphate and polypyrrole to introduce desired functionalities. Polyphosphate reinforces flame retardancy and thermal stability, while polypyrrole imbues the nanocomposite with electrical conductivity and energy storage capabilities [206,207]. Importantly, the chosen polymer matrix plays a critical role in dispersing and stabilising the BP or phosphorene nanosheets, preventing aggregation and oxidation – a crucial factor for long-term performance and processability [208–211]. BP-polymer hybrid nanomaterials, formed by integrating BP or phosphorene with polymers, offer exciting possibilities that extend beyond their individual properties [82]. This approach effectively addresses the inherent stability challenges of BP and phosphorene while capitalising on their unique characteristics. The resulting hybrid nanomaterials exhibit a diverse range of properties and functionalities, making them suitable for a multitude of applications. The exceptional ionic conductivity and electrochemical stability of BP-polymer hybrid nanomaterials make them promising candidates for next-generation battery electrolytes [212]. These electrolytes offer a safe and reliable pathway for ionic conduction, minimising the risk of short circuits within batteries. In the field of biomedicine, BP nanosheets integrated with biocompatible polymers demonstrate enhanced biocompatibility, opening doors for applications in drug delivery, biosensing, and tissue regeneration. Fig. 10a shows an overview of two-dimensional black phosphorus (BP) and hybrid nanomaterials that contain BP nanosheets or quantum dots mixed with polymers, demonstrating their applications. It also discusses the properties, fabrication methods, and wide-ranging applications of two-dimensional black phosphorus [82]. Fig. 10b highlights the multifaceted nature of BP nanosheets, showing their involvement in various applications, especially as part of nanocomposites. It also presents hybrid nanomaterials that incorporate BP nanosheets or quantum dots with polymers, emphasising their diverse range of applications [45].

Black phosphorus (BP) possesses a unique combination of properties that make it highly attractive for various applications. Its high carrier mobility and direct bandgap characteristics render it suitable for high-performance field-effect transistors (FETs) and sensitive photodetectors across the infrared to visible spectrum [213]. Unlike graphene and graphite, BP's finite bandgap makes it particularly advantageous for FETs and optoelectronic devices. Additionally, the anisotropic nature of BP leads to varying electrical, optical, and thermal properties along

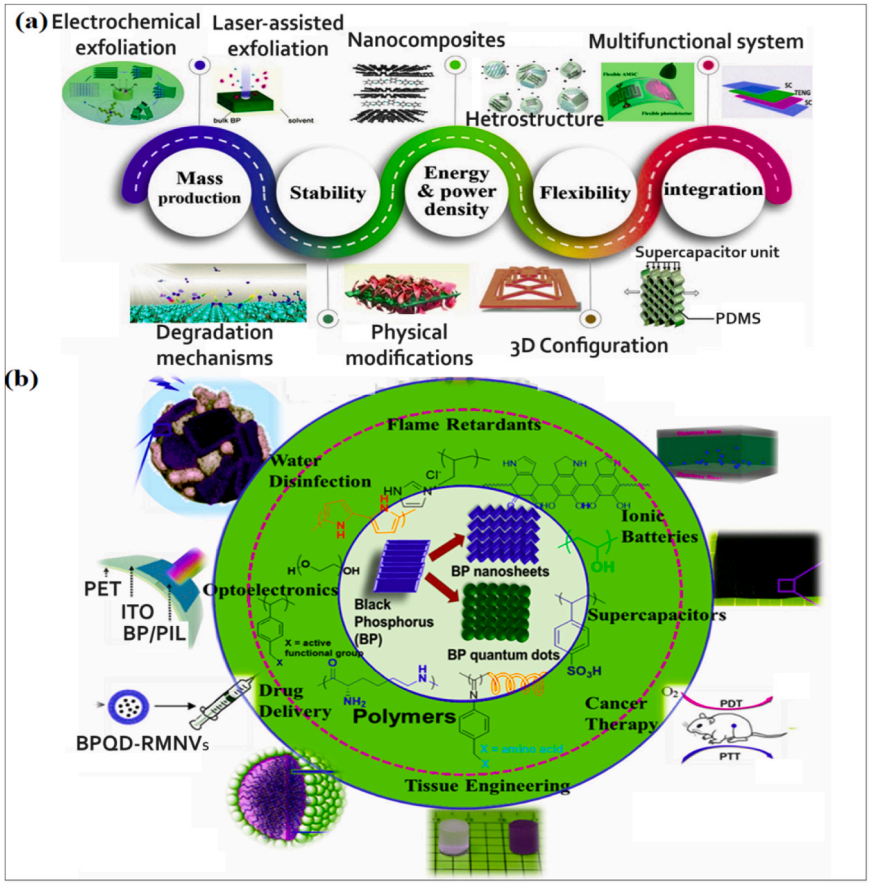

Fig. 10. (a) Two-dimensional black phosphorus: Properties, fabrication, and applications[82], (b) Hybrid nanomaterials comprising black phosphorus (BP) nanosheets or quantum dots integrated with polymers and applications [45].

different crystallographic planes. This anisotropy opens doors for applications in thermoelectric devices and potentially even non-volatile memory [78,214]. The bandgap of BP plays a crucial role in determining its electrical and optical properties. Notably, BP exhibits a unique tunability of its bandgap depending on the number of layers. When exfoliated down to a single layer (phosphorene), BP boasts a wide bandgap near 2 eV, enabling light absorption and emission in the visible spectrum – ideal for optoelectronic applications [215,216]. Conversely, bulk BP (with many layers) possesses a narrow bandgap of around 0.3 eV, corresponding to the infrared range, making it suitable for infrared detectors and thermoelectric devices. This ability to engineer the bandgap by varying layer count offers a significant advantage for designing electronic and optoelectronic devices with tailored properties. Few-layer black phosphorus (FL-BP) presents immense potential due to its exceptional electronic, optical, and mechanical properties. Unlike bulk BP, FL-BP possesses a flexible and tuneable structure, making it adaptable for diverse applications such as flexible electronics, optoelectronic devices, spintronics, and even quantum computing [214,217,218]. Notably, phosphorene, a single layer of BP atoms, stands out within the FL-BP category for its high on/off current ratios and exceptional electrical performance [31,219,220]. Recent advancements have introduced methods for transforming phosphorene into 2D phosphorene oxide (POx) nanoflakes via electro spraying. This technique allows for the production of larger and more sensitive nanostructures compared to conventional exfoliation methods. These POx nanoflakes exhibit promising applications in sensors and actuators due to their observed piezoelectric behaviour under PFM measurements [221]. BP's inherent susceptibility to oxidation presents a hurdle for its long-term stability and device integration. To address this challenge, researchers have explored various functionalisation strategies, including van der Waals heterostructures and metal contacts. For instance, coating BP with multilayer C24 molecules has been shown to effectively prevent degradation, paving the way for advanced electronic and photonic devices based on these heterostructures [213]. Similarly, studies have demonstrated the use of nickel as a contact metal to reduce resistance and enhance the performance of BP-based devices [218]. Beyond its potential for electronic and optoelectronic devices, BP holds promise for revolutionising lithium metal batteries. Researchers have explored integrating BP and phosphorene into polymer composites and electrolytes to address critical challenges in these batteries [222,223]. Optimising BP nanosheets and developing solid polymer electrolytes (SPEs) has demonstrated the possibility of enhancing the capacity, stability, and safety of lithium metal batteries [85,86,200]. Studies have shown that BP nanosheets can be passivated to improve their compatibility with the electrolyte and enhance battery performance (e.g., TEM image). X-ray photoelectron spectroscopy (XPS) analysis can be used to characterise the passivation layer on BP surfaces (e.g., XPS spectra). Furthermore, researchers have developed methods for synthesising BP-incorporated SPEs and analysing their elemental composition (e.g., elemental mapping). Fig. 11 shows the results from these studies, such as the TEM image of passivated BP nanosheets (Fig. 11a), the XPS spectra of P_2p and O_1s signals for bulk BP and its passivated layers (Fig. 11b, c), and the schematic diagrams of the electrolyte synthesis and elemental mapping of the prepared electrolyte solution (Fig. 11d, e) [45].

Researchers have explored integrating BP and phosphorene into polymer composites and electrolytes to address critical challenges in these batteries. Optimising BP nanosheets and developing solid polymer electrolytes (SPEs) has demonstrated the possibility of enhancing the

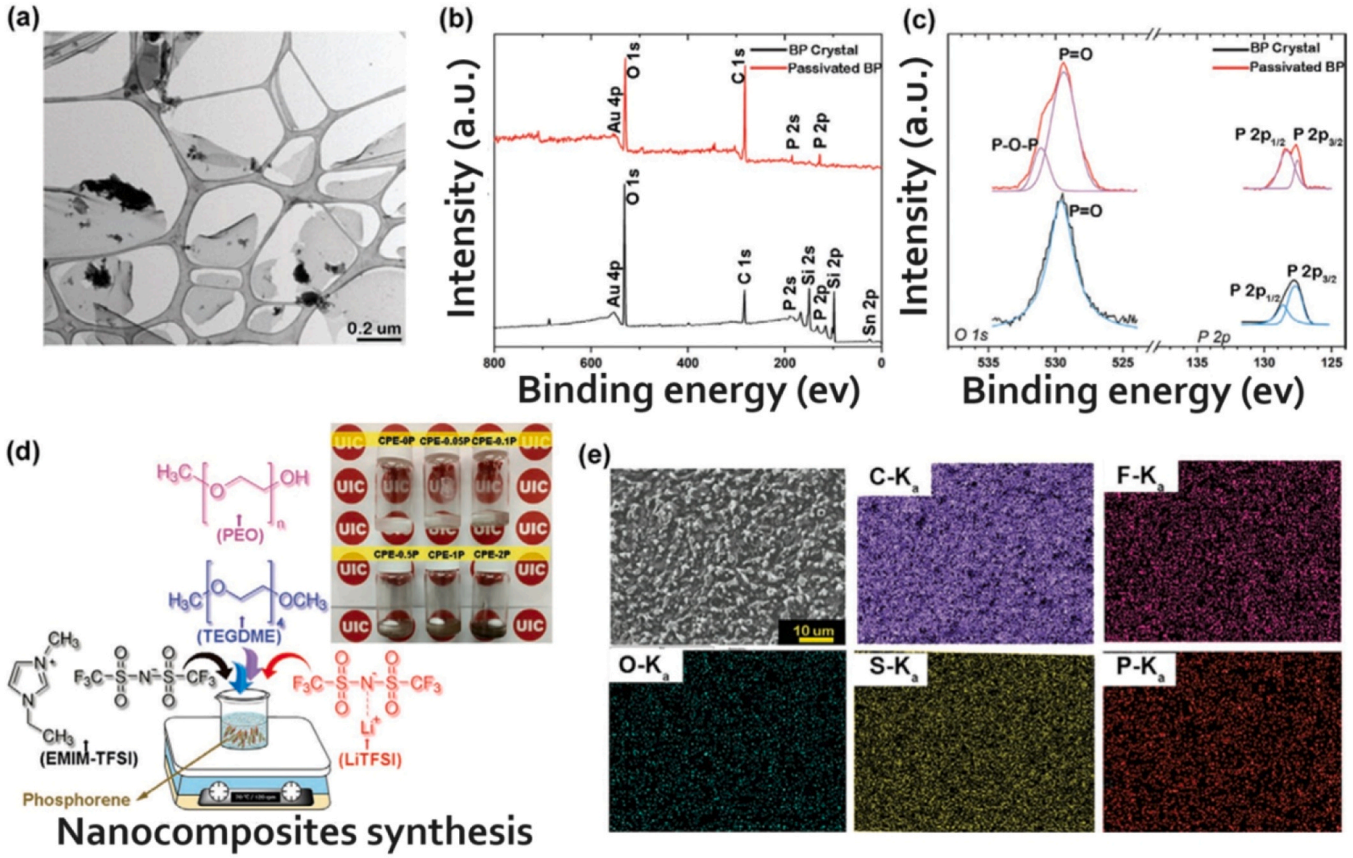

Fig. 11. a) TEM image of passivated BP sheets b) XPS survey spectrum c) XPS spectra of P 2p and O 1 s signal corresponds to bulk BP and its passivated layers in high resolution d) schematic representation of synthesis procedure with inset corresponds to image of prepared electrodes where left to right represents CPE-0 P without any additives and nanocomposite polymer electrolytes consists of 0.05, 0.1, 0.5, 1, and 2 wt% of passivated BP nanosheet e) SEM image representing CPE having passivated BP with 0.5 wt% and its corresponding EDS analysis[45].

capacity, stability, and safety of lithium metal batteries. Electrolyte research plays a pivotal role in advancing battery technologies. A key focus lies in understanding and optimising factors that influence ionic conductivity and electrochemical stability. Studies have explored various strategies to achieve this goal. For instance, researchers have utilised natural halloysite nanotubes to create composite polymer electrolytes, exhibiting enhanced conductivity and suitability for solid-state lithium-ion batteries [224]. Additionally, Ulaganathan et al. [225] successfully synthesised a polymer electrolyte by complexing ethylene carbonate (EC) and propylene carbonate (PC), leading to a significant improvement in ionic conductivity. In another study, Choi et al. [226] investigated the morphological effects of filler materials within solid polymer electrolytes. Their findings revealed that electrolytes containing dendritic fillers exhibited considerably higher ionic conductivities compared to those with spherical fillers. Significantly, incorporating passivated BP nanosheets into the polymer electrolyte has been shown to improve both ionic conductivity and maintain electrochemical stability up to 5 V [85,86]. This approach resulted in a substantial increase in ionic conductivity, with values ranging from $5.9 \times 10{-}4$ S cm^{-1} for the pristine electrolyte to 1.2×10^{-3} and $2.4 \times 10{-}3$ S cm^{-1} for electrolytes containing increasing BP nanosheet concentrations. Electrochemical stability tests revealed a stable window up to 5 V, with an observed peak at 5.5 V attributed to the oxidation of the polymer network. Electrical conductivity measurements, indicative of the insulating properties of the electrolytes, yielded values of –7×10–9 S cm−1, 3×10–9 S cm−1, and $2{\times}10^{-9}$ S cm^{-1} for the pristine and BP-containing electrolytes, respectively. Fig. 12a shows how the ionic conductivity changes with increasing temperature for CPE-0 P, CPE-0.1 P, and CPE-0.5 P, with an inset graph showing the Nyquist plot of the samples at room temperature (25°C). Fig. 12b shows the linear sweep voltammetry as a measure of the electrochemical stability window, and Fig. 12c shows the direct current polarisation tests for measuring the electronic conductivity of the prepared electrolytes [45].

Electrolyte research encompasses various avenues for improving battery performance. Studies have explored diverse strategies to enhance ionic conductivity, electrochemical stability, and intercalation behaviour within battery materials. Of particular interest is the intercalation behaviour of black phosphorus (BP), which depends on its orientation [227]. This characteristic offers opportunities for tailored battery design. Researchers have investigated various approaches for BP-based battery applications, including laser-assisted exfoliation techniques [228] and composite polymer electrolytes encased within porous membranes [229]. Furthermore, in-situ transmission electron microscopy (TEM) has proven valuable for understanding the structural changes that occur during the lithiation process of BP nanoflakes [230]. Fig. 13 explores the structure and intercalation behaviour of ultrathin 2D BP. Fig. 13a shows the crystalline structure of single-layer BP, emphasising covalent bonding in the zigzag and armchair directions, and the puckered network formed by van der Waals interactions. Fig. 13b represents the sample preparation technique used for TEM analysis. Fig. 13c shows the schematic of the in-situ TEM setup designed for the half-cell battery experiment. Fig. 13d-f illustrate the changes in BP nanoflake interlayer spacing and overall volume expansion during lithiation, captured using a cross-sectional view. Fig. 13g provides a magnified view of the intermediate structure within the (002) plane (from the dashed box in Fig. 10e), outlining the changes in interlayer spacing (yellow and red dashed lines). Fig. 10i depicts the volume expansion (top) in the c-direction and the changes in the interlayer spacing of the (002) plane (bottom) throughout the lithiation process [230].

The incorporation of Two-Dimensional Black Phosphorus (2D BP) and phosphorene into polymer composites has opened doors to a plethora of exciting applications. These materials, with their unique properties, offer exceptional adaptability for diverse uses. 2D BP and phosphorene nanocomposites hold promise in various fields, including flame retardancy, gas sensing, and cancer cell detection. Each application leverages the unique characteristics of these materials to achieve enhanced performance or innovative functionalities. For instance, incorporating black phosphorus or phosphorene into flame retardant materials can significantly improve their resistance to burning. In gas sensors, these nanocomposites offer the potential for heightened sensitivity and selectivity in detecting target gases. Similarly, in the realm of cancer cell detection, they provide a platform for developing highly sensitive and specific diagnostic methods, as mentioned in Table 5.

4. Conclusions and future directions

Black phosphorus (BP) and its monolayer form, phosphorene, are two-dimensional materials that have attracted considerable interest due to their unique properties and potential applications in diverse fields. These materials display adjustable bandgaps, which makes them especially suitable for optoelectronic applications like light-emitting diodes (LEDs) that can function at different wavelengths. This versatility enhances their usefulness in electronic applications. In the field of energy storage, BP and phosphorene outperform traditional graphite anodes commonly used in lithium-ion batteries. They offer increased efficiency and durability, leading to improved battery performance and longevity. Their biocompatibility is another significant advantage, allowing for their use in biomedical applications such as targeted drug delivery systems and biosensors. However, challenges such as maintaining

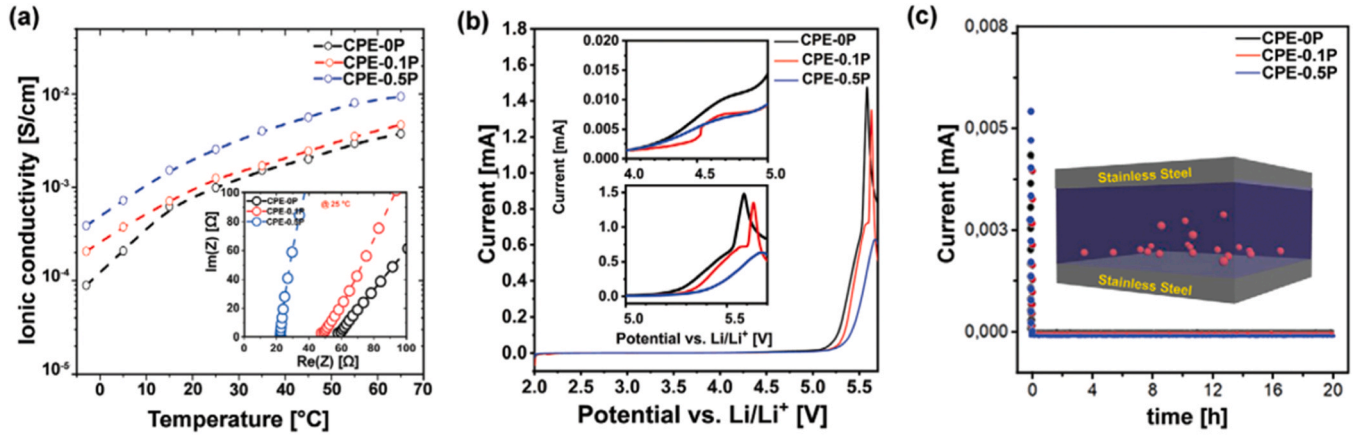

Fig. 12. (a) ionic conductivity with respect to temperature for CPE-0 P, CPE-0.1 P, and CPE-0.5 P. Inset graph representing the Nyquist plot corresponding to samples at a temperature of 25°C, (b) Linear sweep voltammetry representing electrochemical stability window, (c) direct current polarisation tests for measuring electronic conductivity of the prepared electrolytes [45].

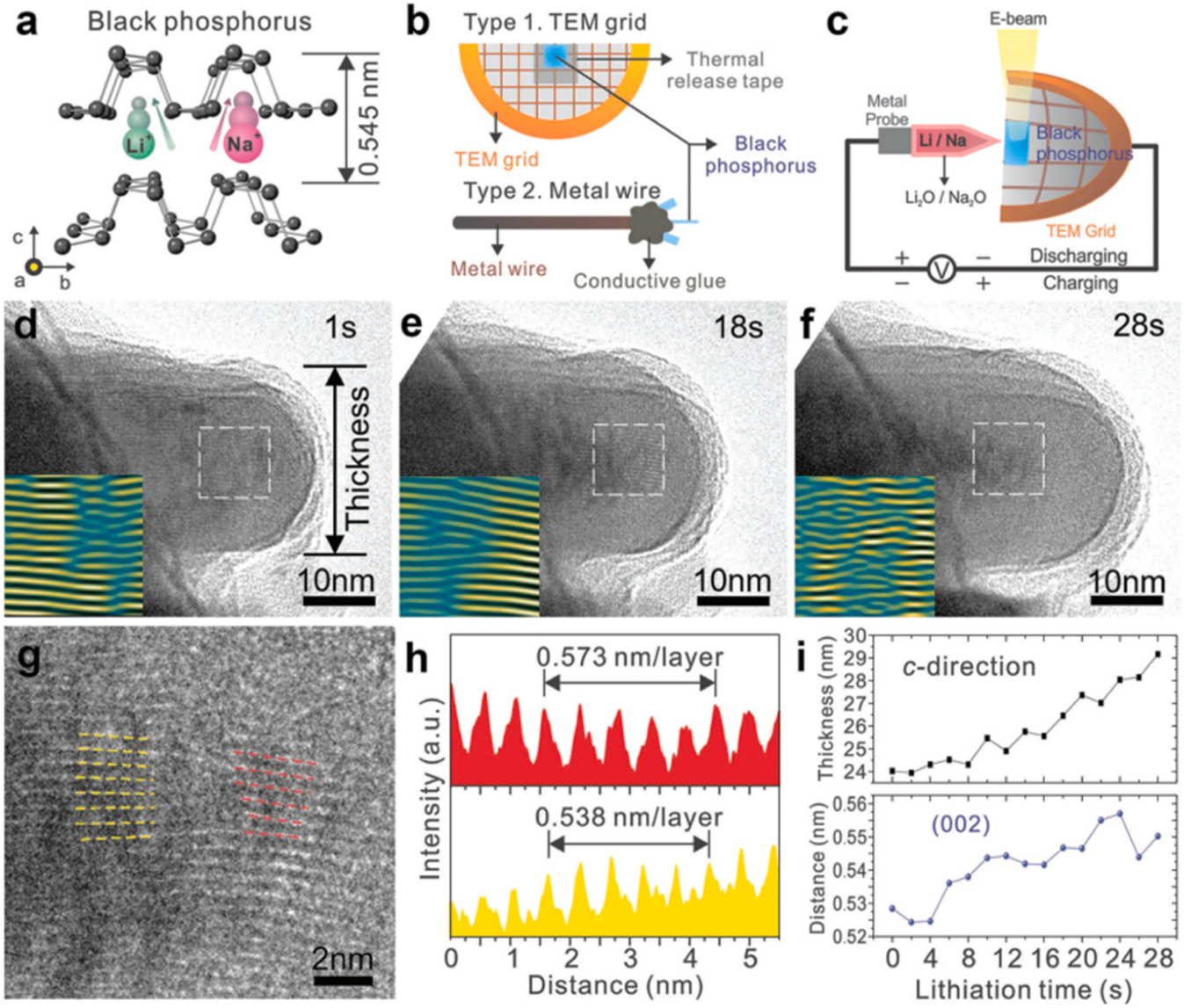

Fig. 13. (a) atomic structure corresponds to single crystalline BP, (b) pictorial representation of sample preparation used for TEM analysis, (c) schematic representation of in-situ TEM setup for half-cell battery, (d-f) time lapse TEM Image which showing the change in interlayer space and volume expansion in BP nanoflakes which is observed through cross-sectional view, (g) enlarged HRTEM image of BP from dashed box in e, (h) (002) plane interlayer spacing given by yellow and red dashed line in g represents the intermediate structure, (i) volume expansion in entire thickness in c-direction (top) and change in interlayer spacing of (002) plane (bottom) during lithiation process [230].

stability under ambient conditions and developing scalable production methods need to be addressed in order to fully exploit their potential. Phosphorene, in particular, shows promise in the fields of energy storage and solar energy conversion. Its unique properties make it an excellent candidate for use in lithium-ion batteries and photovoltaic devices. In lithium-ion batteries, phosphorene can improve performance by offering high capacity, excellent rate capability, and long cycle life. This is attributed to its layered structure, which enables efficient lithium-ion intercalation and deintercalation—a critical process in the operation of these batteries. In photovoltaic devices, phosphorene's adjustable bandgap and high absorption coefficient make it a promising material for solar cells. It has the ability to absorb a wide spectrum of light, which can then be converted into electricity. Despite its remarkable properties and applications, the inherent instability and limited performance of phosphorene pose significant challenges for its practical use. To tackle these issues, researchers have explored various surface modification strategies, such as creating nanocomposites and targeted functionalisation. These methods aim to enhance the stability and performance of phosphorene by combining it with other materials or chemically modifying its surface. For example, integrating phosphorene with other nanomaterials, such as graphene or metal oxides, to create a composite with synergistic effects can enhance its electrical conductivity and stability, making it suitable for energy storage and conversion devices. On the other hand, attaching specific functional groups or molecules to the surface of phosphorene can customise its properties for specific applications. For instance, the introduction of nitrogen can adjust the electronic properties of phosphorene, allowing for the creation of high-performance transistors. Anchoring metal nanoparticles can enhance the catalytic activity of phosphorene, thereby promoting hydrogen evolution and oxygen reduction reactions. Polyethylene glycol (PEG) grafting can improve the biocompatibility of phosphorene, allowing for efficient drug delivery. These surface modification techniques have expanded the application potential of phosphorene in various fields, from electronics to biomedicine. Microtubular BP, with its mesoporous walls, can enhance light trapping and charge separation, which are crucial for photovoltaic conversion. Nano-wrinkled BP films can

Table 5
Comprehensive Summary of Properties and Applications of Black Phosphorus and Phosphorene-based Nanocomposites.

Materials	Properties and Applications	Ref.
Black phosphorus nanosheets, BNTP, epoxy	Enhanced dispersion and synergistic flame retardancy observed in composite materials. Flame retardant polymers for fire safety in various industries.	[36, 231]
Chemically passivated phosphorene, porous triazine-based 2D polymer composites	Enhanced stability, faster sensing, and excellent selectivity. Gas sensing, particularly in the detection of NO_2.	[232]
Long Chain Phosphaphenanthrene Grafted MXene, Black Phosphorene Nanosheets, EVA	Heightened thermal stability and enhanced flame retardancy. EVA nanocomposites for enhanced thermal stability and flame retardancy.	[233]
Black phosphorus, nitrogen-doped carbonised polymer dots composites	Basis for an electrochemical DNA biosensor for specific detection of Escherichia coli O157: H7. DNA biosensors for pathogen detection and targeted analysis.	[234, 235]
Black phosphorus functionalised with melamine-formaldehyde, epoxy	Improved dispersibility, enhanced thermal stability, and flame retardancy. Flame-retardant epoxy nanocomposites.	[236]
Coordination of ruthenium sulfonate ligand with black phosphorus, epoxy	Excellent stability, flame retardancy, and improved thermal conductivity. Flame-retardant epoxy nanocomposites.	[237]
Black phosphorus, polyvinylidene fluoride	Enhanced structural, thermal, electrical, and mechanical performance. PVDF nanocomposites for electronics, energy storage, and multifunctional materials.	[238, 239]
Phosphorene, graphitic carbon nitride	Enhanced hydrogen evolution rates and solar-light-responsive capabilities. Photoelectrochemical water splitting for hydrogen production.	[240]
Black phosphorus, ethylene imine polymer, waterborne polyurethane	Improved mechanical properties and flame retardancy. Flame-retardant waterborne polyurethane (WPU) nanocomposites.	[241]
Sutured layer of black phosphorus, epoxy	Photothermal capability and reduced fire hazards. Epoxy composites for improved energy conversion and fire resistance.	[242]
Trifluoromethanesulfonate Erbium-decorated black phosphorus	Ambient stability, flame retardancy, and enhanced durability. Epoxy resin composites for durable and fire-resistant materials.	[243]
Functionalised/triazine-based covalent organic framework, black phosphorus	Flame retardancy and improved mechanical properties. Epoxy nanocomposites with enhanced fire resistance and mechanical strength.	[198]
Black phosphorus modified MXene with polydopamine coating	Improved mechanical performance, enhanced thermal stability, and flame retardancy. Thermoplastic polyurethane (TPU) for fire-resistant materials.	[244]
Black phosphorus-Ti_3C_2 MXene hybrids	Improved fire safety and enhanced mechanical properties. Water-based coatings and adhesives.	[245]
Black phosphorus covalently grafted with ferrocene oligomer	Smoke suppression and toxicity reduction. Epoxy resin coatings, construction, or electronic devices.	[246, 247]
Montmorillonite-passivated black phosphorus	Improved fire safety and enhanced mechanical properties. Waterborne polyurethane, water-based coatings, adhesives, and structural applications.	[248, 249]
Black phosphorus with tuned defects	High-quality detection of NO and CO. Sensor technology for enhanced sensitivity and accuracy in gas detection.	[250]
Integration of black phosphorus in electrorheological fluid	Tailored phase transition and exfoliation capabilities. Smart electrorheological fluid for thermal management and advanced coatings.	[251, 252]
Conducting polypyrrole, black phosphorene quantum dots, poly (3,4-ethylenedioxythiophene) nanorods	Molecularly imprinted, conductive, and incorporate two-dimensional layered graphene-like quantum dots. Electrochemical sensor for Vitamin C and multifunctional utility in flexible electronics, sensors, and energy storage.	[253]
Phosphorene nanoflakes with phase change materials	Efficient thermal charging and broadband solar absorbance. Solar-thermal energy storage coatings for efficient energy storage.	[254]
Mesoporous graphitic carbon nitride with black phosphorus-gold nanoparticles	Enhanced photocatalytic activity and electrochemical sensing capabilities. Photocatalytic hydrogen evolution and electrochemical detection of paracetamol.	[255]
Black phosphorene, silver nanoparticles, amino-functionalised multi-walled carbon nanotubes	Environmental stability and enhanced electrochemical properties. Environmental monitoring, energy storage, or electrochemical sensing.	[256]
Mesoporous graphitic carbon nitride, black phosphorus, transition metal nanoparticles	Photocatalytic activity through wetness impregnation and chemical reduction processes. Environmental remediation, water purification, sustainable energy production, catalysis, energy storage, or nanoelectronics.	[257]
Black phosphorene, titanium carbide MXene, laser-induced porous graphene, α-naphthalene acetic acid	Flexible electrode with nanozyme characteristics and integrated with machine learning devices. Ultra-trace analysis of α-naphthalene acetic acid residues in farmland environments, agro products biosensing, medical diagnostics, or intelligent devices.	[258]
Poly(l-lactide-co-ε-caprolactone), Laminin, black phosphorus	Ternary nanofiber matrices promoting neuritogenesis and creating optimal microenvironments. Neural tissue engineering and regeneration, biomedical devices, or regenerative medicine.	[259]
Titanium dioxide nanoparticles decorated black phosphorus nanosheets	Large specific surface area and selective detection of ammonia (NH3) at room temperature. Room temperature (18 ± 2 °C) NH_3 sensing, gas detection, and environmental monitoring.	[260]
Two-dimensional black phosphorus-sensitised carbon nitride	Enhanced visible light utilisation and accelerated separation of photo-induced carriers. Photocatalysis, sensing, and energy conversion.	[261]
Black phosphorus nanosheets with polyethyleneimine	Photo isomerisation stability and gas responsiveness in acid-alkali atmospheres. Photo-responsive	[262]

(continued on next page)

Table 5 (*continued*)

Materials	Properties and Applications	Ref.
	gas sensors and photoelectric conversion applications.	
Black phosphorus nanosheets loaded in gelatin-poly(ε-caprolactone) nanofibrous scaffolds	Temperature sensitivity and tissue-healing effects, incorporating photothermal-capable black phosphorus nanosheets. Combinational photothermal/chemotherapy, wound healing, in-situ therapy after melanoma surgery.	[263]
Nickel–Iron Layered Double Hydroxide with gold nanoparticles on black phosphorus nanosheets	High conductivity, electrocatalytic activity, and sensitive detection of diphenylamine (DPA) in food samples. Sensitive and accurate detection of DPA in food samples.	[264]
Black phosphorus, Manganese Dioxide, RhB-encapsulated MnO_2, FITC-labelled Peptide-functionalised BP, R-MnO_2-FBP	Dual-mode capability for monitoring O_2 release, dissociation in acidic and H_2O_2-rich environments. Dual-mode monitoring of O_2 self-supply, enhancing photodynamic therapy (PDT).	[265]

increase contact with the electrolyte, leading to improved capacitance and cycling stability. Composites of BP and metal oxide can efficiently degrade organic pollutants under visible light irradiation due to their enhanced charge transfer and separation. BP/epoxy composites can provide both strength and conductivity, making them ideal for both structural and functional applications. BP/polyvinylidene fluoride (PVDF) composites can display enhanced piezoelectricity, enabling the conversion of mechanical energy into electrical energy. BP/polyethylene oxide (PEO) composites can enhance \lithium-ion conductivity, leading to advanced battery electrodes with high capacity and rate performance. Despite the challenges of scalable synthesis and long-term stability, phosphorene and its derivatives hold significant promise for the development of more efficient and sustainable technologies. Ongoing research efforts are expected to overcome these hurdles and unlock the full potential of this material.

Declaration of Competing Interest

The authors declare that they have no known competing financial interests or personal relationships that could have appeared to influence the work reported in this paper.

References

[1] S.V.S. Prasad, R.K. Mishra, S. Gupta, S.B. Prasad, S. Singh, Introduction, History, and Origin of Two Dimensional (2D) Materials, in: 2021: pp. 1–9. ⟨https://doi.org/10.1007/978-981-16-3322-5_1⟩.

[2] K. Verma, S.H. Siddiki, C.K. Maity, R.K. Mishra, M. Moniruzzaman, Development of reduced graphene oxide (rGO) reinforced poly(lactic) acid/ cellulose nanocrystal composite through melt mixing: Effect of nanofiller on thermal, structural, biodegradation and antibacterial properties, Ind. Crops Prod. 204 (2023), https://doi.org/10.1016/j.indcrop.2023.117307.

[3] H. Liu, Y. Du, Y. Deng, P.D. Ye, Semiconducting black phosphorus: synthesis, transport properties and electronic applications, Chem. Soc. Rev. 44 (2015) 2732–2743, https://doi.org/10.1039/C4CS00257A.

[4] S. Yin, X. Ren, P. Lian, Y. Zhu, Y. Mei, Synergistic effects of black phosphorus/boron nitride nanosheets on enhancing the flame-retardant properties of waterborne polyurethane and its flame-retardant mechanism, Polym. (Basel) 12 (2020), https://doi.org/10.3390/polym12071487.

[5] T. Zhao, C.Y. He, S.Y. Ma, K.W. Zhang, X.Y. Peng, G.F. Xie, J.X. Zhong, A new phase of phosphorus: the missed tricycle type red phosphorene, J. Phys.: Condens. Matter 27 (2015) 265301, https://doi.org/10.1088/0953-8984/27/26/265301.

[6] N. Mohamad Latiff, C.C. Mayorga-Martinez, Z. Sofer, A.C. Fisher, M. Pumera, Cytotoxicity of phosphorus allotropes (black, violet, red,), Appl. Mater. Today 13 (2018) 310–319, https://doi.org/10.1016/j.apmt.2018.09.010.

[7] K.S. Kim, Recent Progress on a Two-Dimensional Semiconductor, Black Phosphorus, Phys. High. Technol. 25 (2016) 31–37, https://doi.org/10.3938/PhiT.25.039.

[8] C. Wang, Y. Huang, X. Duan, Enhanced electrical characteristics of black phosphorus by polyaniline and protonic acid surface doping. 2017 IEEE 17th International Conference on Nanotechnology (IEEE-NANO), IEEE, 2017, pp. 453–455, https://doi.org/10.1109/NANO.2017.8117384.

[9] F. Margot, S. Lisi, I. Cucchi, E. Cappelli, A. Hunter, I. Gutiérrez-Lezama, K. Ma, F. von Rohr, C. Berthod, F. Petocchi, S. Poncé, N. Marzari, M. Gibertini, A. Tamai, A.F. Morpurgo, F. Baumberger, Electronic Structure of Few-Layer Black Phosphorus from μ-ARPES, Nano Lett. 23 (2023) 6433–6439, https://doi.org/10.1021/acs.nanolett.3c01226.

[10] S.H. Park, S. Kwon, Modeling angle-resolved photoemission of graphene and black phosphorus nano structures, Sci. Data 3 (2016), https://doi.org/10.1038/sdata.2016.31.

[11] C. Huang, S. Duan, W. Zhang, High-resolution time- and angle-resolved photoemission studies on quantum materials, Quantum Front. 1 (2022), https://doi.org/10.1007/s44214-022-00013-x.

[12] J. Zhu, J. Shi, A.H. MacDonald, Theory of angle-resolved photoemission spectroscopy in graphene-based moiré superlattices, Phys. Rev. B 103 (2021), https://doi.org/10.1103/physrevb.103.235146.

[13] A.P. Reddy, T. Devakul, L. Fu, Artificial Atoms, Wigner Molecules, and an Emergent Kagome Lattice in Semiconductor Moiré Superlattices, Phys. Rev. Lett. 131 (2023) 246501, https://doi.org/10.1103/PhysRevLett.131.246501.

[14] Y. Liu, C. Zeng, J. Yu, J. Zhong, B. Li, Z. Zhang, Z. Liu, Z.M. Wang, A. Pan, X. Duan, Moiré superlattices and related moiré excitons in twisted van der Waals heterostructures, Chem. Soc. Rev. 50 (2021), https://doi.org/10.1039/d0cs01002b.

[15] C.Q. Han, M.Y. Yao, X.X. Bai, L. Miao, F. Zhu, D.D. Guan, S. Wang, C.L. Gao, C. Liu, D. Qian, Y. Liu, J.F. Jia, Electronic structure of black phosphorus studied by angle-resolved photoemission spectroscopy, Phys. Rev. B Condens Matter Mater. Phys. 90 (2014), https://doi.org/10.1103/PhysRevB.90.085101.

[16] X. Chen, J.S. Ponraj, D. Fan, H. Zhang, An overview of the optical properties and applications of black phosphorus, Nanoscale 12 (2020) 3513–3534, https://doi.org/10.1039/C9NR09122J.

[17] Y. Zhou, J. Chen, L. Yue, D. Ren, Preparation of High-Intensity Fluorescent Black Phosphorus Nanosheets, Phys. Status Solidi (a) 220 (2023), https://doi.org/10.1002/pssa.202200806.

[18] M. Bouatou, R. Harsh, C. Chacon, Y. Girard, V. Repain, A. Bellec, S. Rousset, A. Smogunov, Y.J. Dappe, J. Lagoute, Black Phosphorus for Directed Molecular Assembly with Weak Electronic Coupling, Adv. Mater. Interfaces 8 (2021), https://doi.org/10.1002/admi.202101644.

[19] J. Su, T. Mou, J. Wen, B. Wang, Nondestructive functionalization of monolayer black phosphorus using Lewis acids: A first-principles study, Appl. Surf. Sci. 518 (2020) 146210, https://doi.org/10.1016/j.apsusc.2020.146210.

[20] A. Rabiei Baboukani, I. Khakpour, V. Drozd, C. Wang, Liquid-Based Exfoliation of Black Phosphorus into Phosphorene and Its Application for Energy Storage Devices, Small Struct. 2 (2021), https://doi.org/10.1002/sstr.202000148.

[21] G. Tiouitchi, M.A. Ali, A. Benyoussef, M. Hamedoun, A. Lachgar, A. Kara, A. Ennaoui, A. Mahmoud, F. Boschini, H. Oughaddou, A. El Moutaouakil, A. El Kenz, O. Mounkachi, Efficient production of few-layer black phosphorus by liquid-phase exfoliation, R. Soc. Open Sci. 7 (2020) 201210, https://doi.org/10.1098/rsos.201210.

[22] J.R. Brent, N. Savjani, E.A. Lewis, S.J. Haigh, D.J. Lewis, P. O'Brien, Production of few-layer phosphorene by liquid exfoliation of black phosphorus, Chem. Commun. 50 (2014) 13338–13341, https://doi.org/10.1039/C4CC05752J.

[23] M. Galluzzi, Y. Zhang, X.-F. Yu, Mechanical properties and applications of 2D black phosphorus, J. Appl. Phys. 128 (2020), https://doi.org/10.1063/5.0034893.

[24] A. Khandelwal, K. Mani, M.H. Karigerasi, I. Lahiri, Phosphorene – The two-dimensional black phosphorous: Properties, synthesis and applications, Mater. Sci. Eng.: B 221 (2017) 17–34, https://doi.org/10.1016/j.mseb.2017.03.011.

[25] S. Bagheri, N. Mansouri, E. Aghaie, Phosphorene: A new competitor for graphene, Int J. Hydrog. Energy 41 (2016) 4085–4095, https://doi.org/10.1016/j.ijhydene.2016.01.034.

[26] G. Qu, T. Xia, W. Zhou, X. Zhang, H. Zhang, L. Hu, J. Shi, X.F. Yu, G. Jiang, Property-Activity Relationship of Black Phosphorus at the Nano-Bio Interface: From Molecules to Organisms, Chem. Rev. 120 (2020), https://doi.org/10.1021/acs.chemrev.9b00445.

[27] M.I. Ahamed, N. Shakeel, N. Anwar, Structure and Fundamental Properties of Black Phosphorus, in: 2020: pp. 139–156. ⟨https://doi.org/10.1007/978-3-030-29555-4_7⟩.

[28] S.V. Chekmazov, A.A. Zagitova, A.M. Ionov, S.G. Protasova, V.N. Zverev, A. A. Mazilkin, V.I. Kulakov, S.I. Bozhko, Investigation of Electronic and Atomic Structure and Transport Properties of Black Phosphorus Single Crystals, J. Surf. Investig. 17 (2023), https://doi.org/10.1134/S1027451023030035.

[29] X. Ling, S. Huang, E.H. Hasdeo, L. Liang, W.M. Parkin, Y. Tatsumi, A.R. T. Nugraha, A.A. Puretzky, P.M. Das, B.G. Sumpter, D.B. Geohegan, J. Kong, R. Saito, M. Drndic, V. Meunier, M.S. Dresselhaus, Anisotropic Electron-Photon and Electron-Phonon Interactions in Black Phosphorus, Nano Lett. 16 (2016), https://doi.org/10.1021/acs.nanolett.5b04540.

[30] Q. Wei, X. Peng, Superior mechanical flexibility of phosphorene and few-layer black phosphorus, Appl. Phys. Lett. 104 (2014), https://doi.org/10.1063/1.4885215.

[31] A. Kumar, L. Viscardi, E. Faella, F. Giubileo, K. Intonti, A. Pelella, S. Sleziona, O. Kharsah, M. Schleberger, A. Di Bartolomeo, Black phosphorus unipolar

transistor, memory, and photodetector, J. Mater. Sci. 58 (2023), https://doi.org/10.1007/s10853-023-08169-0.
[32] V. Chaudhary, P. Neugebauer, O. Mounkachi, S. Lahbabi, A. El Fatimy, Phosphorene—an emerging two-dimensional material: recent advances in synthesis, functionalization, and applications, 2d Mater. 9 (2022) 032001, https://doi.org/10.1088/2053-1583/ac6dc2.
[33] A. Yang, D. Wang, X. Wang, D. Zhang, N. Koratkar, M. Rong, Recent advances in phosphorene as a sensing material, Nano Today 20 (2018) 13–32, https://doi.org/10.1016/j.nantod.2018.04.001.
[34] X. Liu, B. Gaihre, M.N. George, Y. Li, M. Tilton, M.J. Yaszemski, L. Lu, 2D phosphorene nanosheets, quantum dots, nanoribbons: synthesis and biomedical applications, Biomater. Sci. 9 (2021) 2768–2803, https://doi.org/10.1039/D0BM01972K.
[35] Y. Zheng, Y. Chen, B. Gao, B. Lin, X. Wang, Phosphorene-Based Heterostructured Photocatalysts, Engineering 7 (2021), https://doi.org/10.1016/j.eng.2021.06.004.
[36] J. Pan, M. Wu, Y. Zheng, H. Chu, X. Liu, S. Liu, J. Zhao, W. Xie, Progressive approximation method toward uniformly-dispersed black phosphorene/epoxy composites, Chem. Eng. J. 476 (2023) 146463, https://doi.org/10.1016/j.cej.2023.146463.
[37] Y. Zeng, Z. Guo, Synthesis and stabilization of black phosphorus and phosphorene: Recent progress and perspectives, IScience 24 (2021) 103116, https://doi.org/10.1016/j.isci.2021.103116.
[38] R. Gui, H. Jin, Z. Wang, J. Li, Black phosphorus quantum dots: Synthesis, properties, functionalized modification and applications, Chem. Soc. Rev. 47 (2018), https://doi.org/10.1039/c8cs00387d.
[39] Y. Zhang, J. Wang, Q. Liu, S. Gu, Z. Sun, P.K. Chu, X. Yu, The electrical, thermal, and thermoelectric properties of black phosphorus, APL Mater. 8 (2020), https://doi.org/10.1063/5.0027244.
[40] Y. Zhang, J. Wang, Q. Liu, S. Gu, Z. Sun, P.K. Chu, X. Yu, The electrical, thermal, and thermoelectric properties of black phosphorus, APL Mater. 8 (2020), https://doi.org/10.1063/5.0027244.
[41] Y. Maruyama, S. Suzuki, K. Kobayashi, S. Tanuma, Synthesis and some properties of black phosphorus single crystals, Phys. B+C. 105 (1981), https://doi.org/10.1016/0378-4363(81)90223-0.
[42] D. Wang, F. Luo, M. Lu, X. Xie, L. Huang, W. Huang, Chemical Vapor Transport Reactions for Synthesizing Layered Materials and Their 2D Counterparts, Small 15 (2019), https://doi.org/10.1002/smll.201804404.
[43] P.K. Tripathy, A. Banerjee, B. Singh, D. Das, A.K. Das, Approaches for Conversion of High Phosphorus Hot Metal to Steel for Flat Products, ISIJ Int. 48 (2008) 578–583, https://doi.org/10.2355/isijinternational.48.578.
[44] G.A. Saenz, D. Fadil, A.B. Kaul, Analysis of multilayer black phosphorus for photodetector applications, in: N.K. Dhar, A.K. Dutta (Eds.), 2017: p. 1020912. ⟨https://doi.org/10.1117/12.2262854⟩.
[45] A. Kumar, D.W. Chang, Towards the Future of Polymeric Hybrids of Two-Dimensional Black Phosphorus or Phosphorene: From Energy to Biological Applications, Polym. (Basel) 15 (2023) 947, https://doi.org/10.3390/polym15040947.
[46] Z. Yang, H. Chen, B. Li, W. Guo, K. Jie, Y. Sun, D. Jiang, I. Popovs, S. Dai, Topotactic Synthesis of Phosphabenzene-Functionalized Porous Organic Polymers: Efficient Ligands in CO_2 Conversion, Angew. Chem. Int. Ed. 58 (2019) 13763–13767, https://doi.org/10.1002/anie.201907015.
[47] A.R. Abdul Rashid, S.H. Ahmad Tarmizi, Synthesis of Graphene based nanocomposites and their application – A Review, Malays. J. Sci. Health Technol. 8 (2022) 51–57, https://doi.org/10.33102/mjosht.v8i2.301.
[48] T. Tomai, Y. Nakayasu, Y. Okamura, S. Ishiguro, N. Tamura, S. Katahira, I. Honma, Bottom-up synthesis of graphene via hydrothermal cathodic reduction, Carbon N. Y 158 (2020) 131–136, https://doi.org/10.1016/j.carbon.2019.11.052.
[49] Y. Tao, S. Kou, Segregation control in vertical Bridgman crystal growth, J. Cryst. Growth 169 (1996) 368–375, https://doi.org/10.1016/S0022-0248(96)00347-8.
[50] X. Mu, J. Wang, M. Sun, Two-dimensional black phosphorus: physical properties and applications, Mater. Today Phys. 8 (2019) 92–111, https://doi.org/10.1016/j.mtphys.2019.02.003.
[51] S. Bhowmik, A.Govind Rajan, Chemical vapor deposition of 2D materials: A review of modeling, simulation, and machine learning studies, IScience 25 (2022) 103832, https://doi.org/10.1016/j.isci.2022.103832.
[52] J.H. Yuan, A. Cresti, K.H. Xue, Y.Q. Song, H.L. Su, L.H. Li, N.H. Miao, Z.M. Sun, J. F. Wang, X.S. Miao, TlP 5: An unexplored direct band gap 2D semiconductor with ultra-high carrier mobility, J. Mater. Chem. C. Mater. 7 (2019), https://doi.org/10.1039/c8tc05164j.
[53] A.K. Tareen, K. Khan, S. Rehman, M. Iqbal, J. Yu, Nasir mahmood, Z. Zhou, J. Yin, Chuan li, H. Zhang, Recent development in emerging phosphorene based novel materials: Progress, challenges, prospects and their fascinating sensing applications, Prog. Solid State Chem. 65 (2022), https://doi.org/10.1016/j.progsolidstchem.2021.100336.
[54] R. Prasannachandran, T.V. Vineesh, A. Anil, B.M. Krishna, M.M. Shaijumon, Functionalized Phosphorene Quantum Dots As Efficient Electrocatalyst for Oxygen Evolution Reaction, ECS Meet. Abstr. MA2019- 01 (2019), https://doi.org/10.1149/ma2019-01/29/1409.
[55] X. Xu, Black phosphorus: a novel 2D material and its photonics applications (Conference Presentation), in: 2018. ⟨https://doi.org/10.1117/12.2286329⟩.
[56] M. Zhao, H. Qian, X. Niu, W. Wang, L. Guan, J. Sha, Y. Wang, Growth Mechanism and Enhanced Yield of Black Phosphorus Microribbons, Cryst. Growth Des. 16 (2016), https://doi.org/10.1021/acs.cgd.5b01709.
[57] Y. Xu, J. Yuan, L. Fei, X. Wang, Q. Bao, Y. Wang, K. Zhang, Y. Zhang, Selenium-Doped Black Phosphorus for High-Responsivity 2D Photodetectors, Small 12 (2016), https://doi.org/10.1002/smll.201600692.
[58] A. Gudimalla, R.K. Mishra, P. Arora, Novel Approaches to Nanomedicine and Nanotechnology, in: Recent Trends in Nanomedicine and Tissue Engineering, River Publishers, New York, 2022, pp. 19–56, https://doi.org/10.1201/9781003339236-2.
[59] K.N. Dinh, Y. Zhang, W. Sun, The synthesis of black phosphorus: From zero: From three-dimensional nanostructures, JPhys Energy 3 (2021), https://doi.org/10.1088/2515-7655/abf2da.
[60] R. Modak, K. Goto, S. Ueda, Y. Miura, K.I. Uchida, Y. Sakuraba, Combinatorial tuning of electronic structure and thermoelectric properties in Co2MnAl1-xSixWeyl semimetals, APL Mater. 9 (2021), https://doi.org/10.1063/5.0041100.
[61] D. Scelta, A. Baldassarre, M. Serrano-Ruiz, K. Dziubek, A.B. Cairns, M. Peruzzini, R. Bini, M. Ceppatelli, Interlayer Bond Formation in Black Phosphorus at High Pressure, Angew. Chem. - Int. Ed. 56 (2017), https://doi.org/10.1002/anie.201708368.
[62] S. Jalaei, J. Karamdel, H. Ghalami-Bavil-Olyaee, Mid-Infrared Photodetector Based on Selenium-Doped Black Phosphorus, Phys. Status Solidi (A) Appl. Mater. Sci. 217 (2020), https://doi.org/10.1002/pssa.202000483.
[63] B. Yang, B. Wan, Q. Zhou, Y. Wang, W. Hu, W. Lv, Q. Chen, Z. Zeng, F. Wen, J. Xiang, S. Yuan, J. Wang, B. Zhang, W. Wang, J. Zhang, B. Xu, Z. Zhao, Y. Tian, Z. Liu, Te-Doped Black Phosphorus Field-Effect Transistors, Adv. Mater. 28 (2016), https://doi.org/10.1002/adma.201603723.
[64] Z. Chen, Y. Zhu, Q. Wang, W. Liu, Y. Cui, X. Tao, D. Zhang, Fibrous phosphorus: A promising candidate as anode for lithium-ion batteries, Electro Acta 295 (2019), https://doi.org/10.1016/j.electacta.2018.10.062.
[65] Y. Zhang, Q. Jiang, P. Lang, N. Yuan, J. Tang, Fabrication and applications of 2D black phosphorus in catalyst, sensing and electrochemical energy storage, J. Alloy. Compd. 850 (2021), https://doi.org/10.1016/j.jallcom.2020.156580.
[66] R. Wang, M. Zhang, B. Ge, L. Zhang, J. Zhou, S. Liu, T. Jiao, Facile preparation of black phosphorus-based rGO-BP-Pd composite hydrogels with enhanced catalytic reduction of 4-nitrophenol performances for wastewater treatment, J. Mol. Liq. 310 (2020), https://doi.org/10.1016/j.molliq.2020.113083.
[67] S.V. Pedersen, F. Muramutsa, J.D. Wood, C. Husko, D. Estrada, B.J. Jaques, Mechanochemical conversion kinetics of red to black phosphorus and scaling parameters for high volume synthesis, NPJ 2D Mater. Appl. 4 (2020), https://doi.org/10.1038/s41699-020-00170-4.
[68] S. Kitada, N. Shimizu, M.Z. Hossain, Safe and Fast Synthesis of Black Phosphorus and Its Purification, ACS Omega 5 (2020), https://doi.org/10.1021/acsomega.0c00404.
[69] Y. Zhao, J. Huang, R. Zhang, Y. Yan, Y. Zhang, Facile and efficient preparation of high-quality black phosphorus quantum dot films for sensing applications, RSC Adv. 10 (2020), https://doi.org/10.1039/c9ra10900e.
[70] Y. Zeng, Z. Guo, Synthesis and stabilization of black phosphorus and phosphorene: recent progress and perspectives, IScience 24 (2021), https://doi.org/10.1016/j.isci.2021.103116.
[71] M. Liu, S. Feng, Y. Hou, S. Zhao, L. Tang, J. Liu, F. Wang, B. Liu, High yield growth and doping of black phosphorus with tunable electronic properties, Mater. Today 36 (2020), https://doi.org/10.1016/j.mattod.2019.12.027.
[72] M. Baba, F. Izumida, Y. Takeda, A. Morita, Preparation of black phosphorus single crystals by a completely closed bismuth-flux method and their crystal morphology, Jpn J. Appl. Phys. 28 (1989), https://doi.org/10.1143/JJAP.28.1019.
[73] Y. Wang, M. He, S. Ma, C. Yang, M. Yu, G. Yin, P. Zuo, Low-Temperature Solution Synthesis of Black Phosphorus from Red Phosphorus: Crystallization Mechanism and Lithium Ion Battery Applications, J. Phys. Chem. Lett. 11 (2020), https://doi.org/10.1021/acs.jpclett.0c00746.
[74] N. Suzuki, M. Aoki, Interplanar forces of black phosphorus caused by electron-lattice interaction, Solid State Commun. 61 (1987), https://doi.org/10.1016/0038-1098(87)90368-1.
[75] P.W. Bridgman, Two new modifications of phosphorus, J. Am. Chem. Soc. 36 (1914), https://doi.org/10.1021/ja02184a002.
[76] C.M. Park, H.J. Sohn, Black phosphorus and its composite for lithium rechargeable batteries, Adv. Mater. 19 (2007), https://doi.org/10.1002/adma.200602592.
[77] M. Köpf, N. Eckstein, D. Pfister, C. Grotz, I. Krüger, M. Greiwe, T. Hansen, H. Kohlmann, T. Nilges, Access and in situ growth of phosphorene-precursor black phosphorus, J. Cryst. Growth 405 (2014), https://doi.org/10.1016/j.jcrysgro.2014.07.029.
[78] L. Kou, C. Chen, S.C. Smith, Phosphorene: Fabrication, Properties, and Applications, J. Phys. Chem. Lett. 6 (2015) 2794–2805, https://doi.org/10.1021/acs.jpclett.5b01094.
[79] S. Wu, K.S. Hui, K.N. Hui, 2D Black Phosphorus: from Preparation to Applications for Electrochemical Energy Storage, Adv. Sci. 5 (2018), https://doi.org/10.1002/advs.201700491.
[80] I. Shirotani, J. Mikami, T. Adachi, Y. Katayama, K. Tsuji, H. Kawamura, O. Shimomura, T. Nakajima, Phase transitions and superconductivity of black phosphorus and phosphorus-arsenic alloys at low temperatures and high pressures, Phys. Rev. B 50 (1994), https://doi.org/10.1103/PhysRevB.50.16274.
[81] M. Pica, R. D'Amato, Chemistry of phosphorene: Synthesis, functionalization and biomedical applications in an update review, Inorg. (Basel) 8 (2020), https://doi.org/10.3390/inorganics8040029.
[82] Y. Wu, W. Yuan, M. Xu, S. Bai, Y. Chen, Z. Tang, C. Wang, Y. Yang, X. Zhang, Y. Yuan, M. Chen, X. Zhang, B. Liu, L. Jiang, Two-dimensional black phosphorus:

Properties, fabrication and application for flexible supercapacitors, Chem. Eng. J. 412 (2021) 128744, https://doi.org/10.1016/j.cej.2021.128744.
[83] V. Paolucci, G. D'Olimpio, L. Lozzi, A.M. Mio, L. Ottaviano, M. Nardone, G. Nicotra, P. Le-Cornec, C. Cantalini, A. Politano, Sustainable Liquid-Phase Exfoliation of Layered Materials with Nontoxic Polarclean Solvent, ACS Sustain Chem. Eng. 8 (2020), https://doi.org/10.1021/acssuschemeng.0c04191.
[84] S. Wu, K.S. Hui, K.N. Hui, 2D Black Phosphorus: from Preparation to Applications for Electrochemical Energy Storage, Adv. Sci. 5 (2018), https://doi.org/10.1002/advs.201700491.
[85] Z. Wen, Z. Zhao, L. Li, Z. Sun, N. Chen, Y. Li, F. Wu, R. Chen, Study on the Interfacial Mechanism of Bisalt Polyether Electrolyte for Lithium Metal Batteries, Adv. Funct. Mater. 32 (2022), https://doi.org/10.1002/adfm.202109184.
[86] A. Rocco, A polymeric solid electrolyte based on a poly(ethylene oxide)/poly (bisphenol A-co-epichlorohydrin) blend with LiClO4, Solid State Ion.-. 166 (2004) 115–126, https://doi.org/10.1016/j.ssi.2003.10.015.
[87] C. Subbu, S. Rajendran, K. Kesavan, R. Premila, The physical and electrochemical properties of poly(vinylidene chloride-co-acrylonitrile)-based polymer electrolytes prepared with different plasticizers, Ion. (Kiel.) 22 (2016) 229–240, https://doi.org/10.1007/s11581-015-1535-7.
[88] Chen, S.Y., Yuan, C.Y., Li, W.J., & Chen-Yang, Y.W. (2006, March). Organic-inorganic composite polymer electrolytes based on poly (ethylene glycol)-bridged polysilsesquioxane. In ABSTRACTS OF PAPERS OF THE AMERICAN CHEMICAL SOCIETY (Vol. 231). 1155 16TH ST, NW, WASHINGTON, DC 20036 USA: AMER CHEMICAL SOC., (n.d.).
[89] G. Lee, J.Y. Lee, G.H. Lee, J. Kim, Tuning the thickness of black phosphorus: Via ion bombardment-free plasma etching for device performance improvement, J. Mater. Chem. C. Mater. 4 (2016), https://doi.org/10.1039/c6tc01514j.
[90] J. Pei, X. Gai, J. Yang, X. Wang, Z. Yu, D.Y. Choi, B. Luther-Davies, Y. Lu, Producing air-stable monolayers of phosphorene and their defect engineering, Nat. Commun. 7 (2016), https://doi.org/10.1038/ncomms10450.
[91] M. Schütz, L. Maschio, A.J. Karttunen, D. Usvyat, Exfoliation Energy of Black Phosphorus Revisited: A Coupled Cluster Benchmark, J. Phys. Chem. Lett. 8 (2017), https://doi.org/10.1021/acs.jpclett.7b00253.
[92] K. Yan, H.W. Lee, T. Gao, G. Zheng, H. Yao, H. Wang, Z. Lu, Y. Zhou, Z. Liang, Z. Liu, S. Chu, Y. Cui, Ultrathin two-dimensional atomic crystals as stable interfacial layer for improvement of lithium metal anode, Nano Lett. 14 (2014), https://doi.org/10.1021/nl503125u.
[93] Z. Guo, H. Zhang, S. Lu, Z. Wang, S. Tang, J. Shao, Z. Sun, H. Xie, H. Wang, X. F. Yu, P.K. Chu, From black phosphorus to phosphorene: basic solvent exfoliation, evolution of raman scattering, and applications to ultrafast photonics, Adv. Funct. Mater. 25 (2015), https://doi.org/10.1002/adfm.201502902.
[94] L. Guan, B. Xing, X. Niu, D. Wang, Y. Yu, S. Zhang, X. Yan, Y. Wang, J. Sha, Metal-assisted exfoliation of few-layer black phosphorus with high yield, Chem. Commun. 54 (2018), https://doi.org/10.1039/c7cc08488a.
[95] Y. Song, S. Chang, S. Gradecak, J. Kong, Visibly-transparent organic solar cells on flexible substrates with all-graphene electrodes, Adv. Energy Mater. 6 (2016), https://doi.org/10.1002/aenm.201600847.
[96] Y. Liu, A.A. Elzatahry, W. Luo, K. Lan, P. Zhang, J. Fan, Y. Wei, C. Wang, Y. Deng, G. Zheng, F. Zhang, Y. Tang, L. Mai, D. Zhao, Surfactant-templating strategy for ultrathin mesoporous TiO2 coating on flexible graphitized carbon supports for high-performance lithium-ion battery, Nano Energy 25 (2016), https://doi.org/10.1016/j.nanoen.2016.04.028.
[97] J.D. Wood, S.A. Wells, D. Jariwala, K.S. Chen, E. Cho, V.K. Sangwan, X. Liu, L. J. Lauhon, T.J. Marks, M.C. Hersam, Effective passivation of exfoliated black phosphorus transistors against ambient degradation, Nano Lett. 14 (2014), https://doi.org/10.1021/nl5032293.
[98] P. Yasaei, B. Kumar, T. Foroozan, C. Wang, M. Asadi, D. Tuschel, J.E. Indacochea, R.F. Klie, A. Salehi-Khojin, High-Quality Black Phosphorus Atomic Layers by Liquid-Phase Exfoliation, Adv. Mater. 27 (2015), https://doi.org/10.1002/adma.201405150.
[99] W. Zhao, Z. Xue, J. Wang, J. Jiang, X. Zhao, T. Mu, Large-scale, highly efficient, and green liquid-exfoliation of black phosphorus in ionic liquids, ACS Appl. Mater. Interfaces 7 (2015), https://doi.org/10.1021/acsami.5b10734.
[100] J. Kang, J.D. Wood, S.A. Wells, J.-H. Lee, X. Liu, K.-S. Chen, M.C. Hersam, Solvent Exfoliation of Electronic-Grade, Two-Dimensional Black Phosphorus, ACS Nano 9 (2015) 3596–3604, https://doi.org/10.1021/acsnano.5b01143.
[101] V. Sresht, A.A.H. Pádua, D. Blankschtein, Liquid-phase exfoliation of phosphorene: design rules from molecular dynamics simulations, ACS Nano 9 (2015), https://doi.org/10.1021/acsnano.5b02683.
[102] V.V. Chaban, E.E. Fileti, O.V. Prezhdo, Imidazolium ionic liquid mediates black phosphorus exfoliation while preventing phosphorene decomposition, ACS Nano 11 (2017), https://doi.org/10.1021/acsnano.7b03074.
[103] M.B. Erande, M.S. Pawar, D.J. Late, Humidity Sensing and Photodetection Behavior of Electrochemically Exfoliated Atomically Thin-Layered Black Phosphorus Nanosheets, ACS Appl. Mater. Interfaces 8 (2016), https://doi.org/10.1021/acsami.5b10247.
[104] A. Ambrosi, Z. Sofer, M. Pumera, Electrochemical Exfoliation of Layered Black Phosphorus into Phosphorene, Angew. Chem. Int. Ed. 56 (2017) 10443–10445, https://doi.org/10.1002/anie.201705071.
[105] W. Luo, R. Yang, J. Liu, Y. Zhao, W. Zhu, G. Xia, Thermal sublimation: a scalable and controllable thinning method for the fabrication of few-layer black phosphorus, Nanotechnology 28 (2017), https://doi.org/10.1088/1361-6528/aa76ae.
[106] Z. Huang, H. Hou, Y. Zhang, C. Wang, X. Qiu, X. Ji, Layer-Tunable Phosphorene Modulated by the Cation Insertion Rate as a Sodium-Storage Anode, Adv. Mater. 29 (2017), https://doi.org/10.1002/adma.201702372.
[107] P. Zhang, F. Wang, S. Yang, G. Wang, M. Yu, X. Feng, Flexible in-plane micro-supercapacitors: Progresses and challenges in fabrication and applications, Energy Storage Mater. 28 (2020) 160–187, https://doi.org/10.1016/j.ensm.2020.02.029.
[108] M. El Hammoumi, V. Chaudhary, P. Neugebauer, A. El Fatimy, Chemical vapor deposition: a potential tool for wafer scale growth of two-dimensional layered materials, J. Phys. D. Appl. Phys. 55 (2022) 473001, https://doi.org/10.1088/1361-6463/ac928d.
[109] J.D. Yao, Z.Q. Zheng, G.W. Yang, Production of large-area 2D materials for high-performance photodetectors by pulsed-laser deposition, Prog. Mater. Sci. 106 (2019), https://doi.org/10.1016/j.pmatsci.2019.100573.
[110] A. Zhang, Z. Wang, H. Ouyang, W. Lyu, J. Sun, Y. Cheng, B. Fu, Recent progress of two-dimensional materials for ultrafast photonics, Nanomaterials 11 (2021), https://doi.org/10.3390/nano11071778.
[111] X. Liu, J.D. Wood, K.S. Chen, E. Cho, M.C. Hersam, In situ thermal decomposition of exfoliated two-dimensional black phosphorus, J. Phys. Chem. Lett. 6 (2015), https://doi.org/10.1021/acs.jpclett.5b00043.
[112] Z. Yang, J. Hao, S. Yuan, S. Lin, H.M. Yau, J. Dai, S.P. Lau, Field-Effect Transistors Based on Amorphous Black Phosphorus Ultrathin Films by Pulsed Laser Deposition, Adv. Mater. 27 (2015), https://doi.org/10.1002/adma.201500990.
[113] X. Li, B. Deng, X. Wang, S. Chen, M. Vaisman, S.I. Karato, G. Pan, M.L. Lee, J. Cha, H. Wang, F. Xia, Synthesis of thin-film black phosphorus on a flexible substrate, 2d Mater. 2 (2015), https://doi.org/10.1088/2053-1583/2/3/031002.
[114] T. Niu, New properties with old materials: Layered black phosphorous, Nano Today 12 (2017), https://doi.org/10.1016/j.nantod.2016.08.013.
[115] Y. Zhao, H. Wang, H. Huang, Q. Xiao, Y. Xu, Z. Guo, H. Xie, J. Shao, Z. Sun, W. Han, X.F. Yu, P. Li, P.K. Chu, Surface Coordination of Black Phosphorus for Robust Air and Water Stability, Angew. Chem. - Int. Ed. 55 (2016), https://doi.org/10.1002/anie.201512038.
[116] C. Li, Y. Wu, B. Deng, Y. Xie, Q. Guo, S. Yuan, X. Chen, M. Bhuiyan, Z. Wu, K. Watanabe, T. Taniguchi, H. Wang, J.J. Cha, M. Snure, Y. Fei, F. Xia, Synthesis of Crystalline Black Phosphorus Thin Film on Sapphire, Adv. Mater. 30 (2018), https://doi.org/10.1002/adma.201703748.
[117] X. Ren, J. Zhou, X. Qi, Y. Liu, Z. Huang, Z. Li, Y. Ge, S.C. Dhanabalan, J.S. Ponraj, S. Wang, J. Zhong, H. Zhang, Few-Layer Black Phosphorus Nanosheets as Electrocatalysts for Highly Efficient Oxygen Evolution Reaction, Adv. Energy Mater. 7 (2017), https://doi.org/10.1002/aenm.201700396.
[118] T. Zhang, Y. Wan, H. Xie, Y. Mu, P. Du, D. Wang, X. Wu, H. Ji, L. Wan, Degradation Chemistry and Stabilization of Exfoliated Few-Layer Black Phosphorus in Water, J. Am. Chem. Soc. 140 (2018), https://doi.org/10.1021/jacs.8b02156.
[119] N. Sultana, A. Degg, S. Upadhyaya, T. Nilges, N. Sen Sarma, Synthesis, modification, and application of black phosphorus, few-layer black phosphorus (FLBP), and phosphorene: a detailed review, Mater. Adv. 3 (2022) 5557–5574, https://doi.org/10.1039/D1MA01101D.
[120] X.X. Fu, Y. Niu, Z.W. Hao, M.M. Dong, C.K. Wang, Surface decoration of phosphorene nanoribbons with 4d transition metal atoms for spintronics, Phys. Chem. Chem. Phys. 22 (2020), https://doi.org/10.1039/d0cp02101f.
[121] M. Akhtar, G. Anderson, R. Zhao, A. Alruqi, J.E. Mroczkowska, G. Sumanasekera, J.B. Jasinski, Recent advances in synthesis, properties, and applications of phosphorene, NPJ 2D Mater. Appl. 1 (2017), https://doi.org/10.1038/s41699-017-0007-5.
[122] M.C. Hersam, Invited) Processing and Applications of Monodisperse Two-Dimensional Nanomaterial Inks, ECS Meet. Abstr. MA2017- 01 (2017), https://doi.org/10.1149/ma2017-01/12/796.
[123] A. Castellanos-Gomez, L. Vicarelli, E. Prada, J.O. Island, K.L. Narasimha-Acharya, S.I. Blanter, D.J. Groenendijk, M. Buscema, G.A. Steele, J.V. Alvarez, H. W. Zandbergen, J.J. Palacios, H.S.J. Van Der Zant, Isolation and characterization of few-layer black phosphorus, 2d Mater. 1 (2014), https://doi.org/10.1088/2053-1583/1/2/025001.
[124] H. Liu, A.T. Neal, Z. Zhu, Z. Luo, X. Xu, D. Tománek, P.D. Ye, Phosphorene: An unexplored 2D semiconductor with a high hole mobility, ACS Nano 8 (2014), https://doi.org/10.1021/nn501226z.
[125] H. Liu, A.T. Neal, Z. Zhu, Z. Luo, X. Xu, D. Tománek, Supplementary Material for Phosphorene: A Unexplored 2D Semiconductor with a High Hole Mobility Table of Contents, ACS Nano 20 (1996).
[126] L. Kou, T. Frauenheim, C. Chen, Phosphorene as a superior gas sensor: Selective adsorption and distinct i - V response, J. Phys. Chem. Lett. 5 (2014), https://doi.org/10.1021/jz501188k.
[127] H. Huang, M. Gao, Y. Kang, J. Li, J. Wang, L. Wu, P.K. Chu, Y. Huang, M.R. Ibarra, X.F. Yu, Rapid and scalable production of high-quality phosphorene by plasma-liquid technology, Chem. Commun. 56 (2019), https://doi.org/10.1039/c9cc07640a.
[128] M. Batmunkh, M. Bat-Erdene, J.G. Shapter, Phosphorene and Phosphorene-Based Materials – Prospects for Future Applications, Adv. Mater. 28 (2016), https://doi.org/10.1002/adma.201602254.
[129] N. Han, N. Gao, J. Zhao, Initial Growth Mechanism of Blue Phosphorene on Au (111) Surface, J. Phys. Chem. C. 121 (2017), https://doi.org/10.1021/acs.jpcc.7b04209.
[130] H. Xu, X. Han, Z. Li, W. Liu, X. Li, J. Wu, Z. Guo, H. Liu, Epitaxial Growth of Few-Layer Black Phosphorene Quantum Dots on Si Substrates, Adv. Mater. Interfaces 5 (2018), https://doi.org/10.1002/admi.201801048.
[131] C.P. Bartus, T. Hegedűs, G. Kozma, I. Szenti, R. Vajtai, Z. Kónya, Á. Kukovecz, Exfoliation of black phosphorus in isopropanol-water cosolvents, J. Mol. Struct. 1260 (2022), https://doi.org/10.1016/j.molstruc.2022.132862.

[132] M. Serrano-Ruiz, M. Caporali, A. Ienco, V. Piazza, S. Heun, M. Peruzzini, The role of water in the preparation and stabilization of high-quality phosphorene flakes, Adv. Mater. Interfaces 3 (2016), https://doi.org/10.1002/admi.201500441.
[133] H. Guo, W. Chu, O.V. Prezhdo, Q. Zheng, J. Zhao, Strong Modulation of band gap, carrier mobility and lifetime in two-dimensional black phosphorene through acoustic phonon Excitation, J. Phys. Chem. Lett. 12 (2021) 3960–3967, https://doi.org/10.1021/acs.jpclett.1c00747.
[134] P.K. Sarswat, S. Sarkar, J. Cho, D. Bhattacharyya, M.L. Free, Structural and electrical irregularities caused by selected dopants in black-phosphorus, ECS J. Solid State Sci. Technol. 5 (2016), https://doi.org/10.1149/2.0061611jss.
[135] J. Sun, H.-W. Lee, M. Pasta, H. Yuan, G. Zheng, Y. Sun, Y. Li, Y. Cui, A phosphorene–graphene hybrid material as a high-capacity anode for sodium-ion batteries, Nat. Nanotechnol. 10 (2015) 980–985, https://doi.org/10.1038/nnano.2015.194.
[136] Y. Zhao, H. Wang, X. Yu, Progress of fabrication and surface modification of 2D black phosphorus, Chin. Sci. Bull. 62 (2017) 2252–2261, https://doi.org/10.1360/N972016-01219.
[137] L. Liang, J. Wang, W. Lin, B.G. Sumpter, V. Meunier, M. Pan, Electronic Bandgap and Edge Reconstruction in Phosphorene Materials, Nano Lett. 14 (2014) 6400–6406, https://doi.org/10.1021/nl502892t.
[138] G. Wang, R. Pandey, S.P. Karna, Phosphorene oxide: stability and electronic properties of a novel two-dimensional material, Nanoscale 7 (2015) 524–531, https://doi.org/10.1039/C4NR05384B.
[139] F.T. Johra, W.-G. Jung, Synthesis of Black Phosphorus via a Facile Vapor Transfer Method, Electron. Mater. Lett. 15 (2019) 639–644, https://doi.org/10.1007/s13391-019-00162-7.
[140] K. Abe, N.W. Ashcroft, Crystalline diborane at high pressures, Phys. Rev. B 84 (2011) 104118, https://doi.org/10.1103/PhysRevB.84.104118.
[141] M.F. Tai, W.N. Wang, H.C. Ku, Bulk Superconductivity in the New Orthorhombic (Tl, Pb)-Ca-Sr-Cu-O System, Jpn J. Appl. Phys. 27 (1988) L2287, https://doi.org/10.1143/JJAP.27.L2287.
[142] J. Cheng, L. Gao, T. Li, S. Mei, C. Wang, B. Wen, W. Huang, C. Li, G. Zheng, H. Wang, H. Zhang, Two-Dimensional Black Phosphorus Nanomaterials: Emerging Advances in Electrochemical Energy Storage Science, Nanomicro Lett. 12 (2020), https://doi.org/10.1007/s40820-020-00510-5.
[143] K. Cho, J. Yang, Y. Lu, Phosphorene: An emerging 2D material, J. Mater. Res 32 (2017) 2839–2847, https://doi.org/10.1557/jmr.2017.71.
[144] X. Li, Pressure-induced phase transitions and superconductivity in a black phosphorus single crystal, Acta Crystallogr A Found. Adv. 77 (2021), https://doi.org/10.1107/s0108767321091406.
[145] X. Li, J. Sun, P. Shahi, M. Gao, A.H. MacDonald, Y. Uwatoko, T. Xiang, J. B. Goodenough, J. Cheng, J. Zhou, Pressure-induced phase transitions and superconductivity in a black phosphorus single crystal, Proc. Natl. Acad. Sci. USA 115 (2018), https://doi.org/10.1073/pnas.1810726115.
[146] R. Zhang, J. Waters, A.K. Geim, I.V. Grigorieva, Intercalant-independent transition temperature in superconducting black phosphorus, Nat. Commun. 8 (2017), https://doi.org/10.1038/ncomms15036.
[147] A. Kundu, D. Tristant, N. Sheremetyeva, A. Yoshimura, A. Torres Dias, K.S. Hazra, V. Meunier, P. Puech, Reversible Pressure-Induced Partial Phase Transition in Few-Layer Black Phosphorus, Nano Lett. 20 (2020), https://doi.org/10.1021/acs.nanolett.0c01784.
[148] G. Xiao, Y. Cao, G. Qi, L. Wang, Q. Zeng, C. Liu, Z. Ma, K. Wang, X. Yang, Y. Sui, W. Zheng, B. Zou, Compressed few-layer black phosphorus nanosheets from semiconducting to metallic transition with the highest symmetry, Nanoscale 9 (2017), https://doi.org/10.1039/c7nr03367b.
[149] J. Qiao, X. Kong, Z.-X. Hu, F. Yang, W. Ji, High-mobility transport anisotropy and linear dichroism in few-layer black phosphorus, Nat. Commun. 5 (2014) 4475, https://doi.org/10.1038/ncomms5475.
[150] F. Xia, H. Wang, Y. Jia, Rediscovering black phosphorus as an anisotropic layered material for optoelectronics and electronics, Nat. Commun. 5 (2014) 4458, https://doi.org/10.1038/ncomms5458.
[151] N. Mao, S. Zhang, J. Wu, H. Tian, J. Wu, H. Xu, H. Peng, L. Tong, J. Zhang, Investigation of black phosphorus as a nano-optical polarization element by polarized Raman spectroscopy, Nano Res 11 (2018), https://doi.org/10.1007/s12274-017-1690-4.
[152] J. Kim, J.U. Lee, J. Lee, H.J. Park, Z. Lee, C. Lee, H. Cheong, Anomalous polarization dependence of Raman scattering and crystallographic orientation of black phosphorus, Nanoscale 7 (2015), https://doi.org/10.1039/c5nr04349b.
[153] Y. Zhu, W. Zheng, W. Wang, S. Zhu, L. Li, L. Cheng, M. Jin, Y. Ding, F. Huang, Raman tensor of layered black phosphorus, PhotoniX 1 (2020), https://doi.org/10.1186/s43074-020-00017-7.
[154] Y. Du, C. Ouyang, S. Shi, M. Lei, Ab initio studies on atomic and electronic structures of black phosphorus, J. Appl. Phys. 107 (2010), https://doi.org/10.1063/1.3386509.
[155] B. Deng, R. Frisenda, C. Li, X. Chen, A. Castellanos-Gomez, F. Xia, Progress on Black Phosphorus Photonics, Adv. Opt. Mater. 6 (2018), https://doi.org/10.1002/adom.201800365.
[156] L. Schue, F.A. Goudreault, A. Righi, G.C. Resende, V. Lefebvre, E. Godbout, M. A. Pimenta, M. Cote, S. Francoeur, R. Martel, Out-of-Plane Polarized Visible Luminescence and Electronic Resonance in Black Phosphorus, 852–852, ECS Meet. Abstr. MA2022- 01 (2022), https://doi.org/10.1149/MA2022-0112852mtgabs.
[157] S. Park, S. Woo, H. Min, Semiclassical Boltzmann transport theory of few-layer black phosphorus in various phases, 2d Mater. 6 (2019) 025016, https://doi.org/10.1088/2053-1583/ab01c3.
[158] F. Xia, H. Wang, Y. Jia, Rediscovering black phosphorus as an anisotropic layered material for optoelectronics and electronics, Nat. Commun. 5 (2014) 4458, https://doi.org/10.1038/ncomms5458.
[159] R. Irshad, K. Tahir, B. Li, Z. Sher, J. Ali, S. Nazir, A revival of 2D materials, phosphorene: Its application as sensors, J. Ind. Eng. Chem. 64 (2018) 60–69, https://doi.org/10.1016/j.jiec.2018.03.010.
[160] J.L. Zhang, C. Han, Z. Hu, L. Wang, L. Liu, A.T.S. Wee, W. Chen, 2D Phosphorene: Epitaxial Growth and Interface Engineering for Electronic Devices, Adv. Mater. 30 (2018), https://doi.org/10.1002/adma.201802207.
[161] F. Luo, D. Wang, J. Zhang, X. Li, D. Liu, H. Li, M. Lu, X. Xie, L. Huang, W. Huang, Ultrafast Cathodic Exfoliation of Few-Layer Black Phosphorus in Aqueous Solution, ACS Appl. Nano Mater. 2 (2019), https://doi.org/10.1021/acsanm.9b00667.
[162] H. Liu, P. Lian, Q. Zhang, Y. Yang, Y. Mei, The preparation of holey phosphorene by electrochemical assistance, Electrochem Commun. 98 (2019) 124–128, https://doi.org/10.1016/j.elecom.2018.12.007.
[163] F. Xia, H. Wang, Y. Jia, Rediscovering black phosphorus as an anisotropic layered material for optoelectronics and electronics, Nat. Commun. 5 (2014), https://doi.org/10.1038/ncomms5458.
[164] V. Eswaraiah, Q. Zeng, Y. Long, Z. Liu, Black Phosphorus Nanosheets: Synthesis, Characterization and Applications, Small (2016), https://doi.org/10.1002/smll.201600032.
[165] V. Eswaraiah, Q. Zeng, Y. Long, Z. Liu, Black Phosphorus Nanosheets: Synthesis, Characterization and Applications, Small 12 (2016) 3480–3502, https://doi.org/10.1002/smll.201600032.
[166] V. Christiansson, F. Petocchi, P. Werner, Superconductivity in black phosphorus and the role of dynamical screening, Phys. Rev. B 105 (2022), https://doi.org/10.1103/PhysRevB.105.174513.
[167] S. An, H. Park, M. Kim, Recent advances in single crystal narrow band-gap semiconductor nanomembranes and their flexible optoelectronic device applications: Ge, GeSn, InGaAs, and 2D materials, J. Mater. Chem. C. Mater. 11 (2023) 2430–2448, https://doi.org/10.1039/D2TC05041B.
[168] A. Ng, T.E. Sutto, Y. Deng, R.M. Stroud, T.H. Brintlinger, P.D. Ye, N.D. Bassim, S) TEM Characterization of Chemically Exfoliated Black Phosphorus, Microsc. Microanal. 22 (2016) 1544–1545, https://doi.org/10.1017/S1431927616008564.
[169] Y. Lee, J.Y. Yoon, D. Scullion, J. Jang, E.J.G. Santos, H.Y. Jeong, K. Kim, Atomic-scale imaging of few-layer black phosphorus and its reconstructed edge, J. Phys. D. Appl. Phys. 50 (2017), https://doi.org/10.1088/1361-6463/aa5583.
[170] E. Bonera, A. Molle, Optothermal Raman Spectroscopy of Black Phosphorus on a Gold Substrate, Nanomaterials 12 (2022), https://doi.org/10.3390/nano12091410.
[171] B. Joseph, S. Caramazza, F. Capitani, T. Clarté, F. Ripanti, P. Lotti, A. Lausi, D. Di Castro, P. Postorino, P. Dore, Coexistence of pressure-induced structural phases in bulk black phosphorus: A combined x-ray diffraction and Raman study up to 18 GPa, J. Phys. Condens. Matter 30 (2018), https://doi.org/10.1088/1361-648X/aaebe5.
[172] L. Henry, V. Svitlyk, M. Mezouar, D. Sifré, G. Garbarino, M. Ceppatelli, M. Serrano-Ruiz, M. Peruzzini, F. Datchi, Anisotropic thermal expansion of black phosphorus from nanoscale dynamics of phosphorene layers, Nanoscale 12 (2020), https://doi.org/10.1039/c9nr09218h.
[173] W. Luo, D.Y. Zemlyanov, C.A. Milligan, Y. Du, L. Yang, Y. Wu, P.D. Ye, Surface chemistry of black phosphorus under a controlled oxidative environment, Nanotechnology 27 (2016), https://doi.org/10.1088/0957-4484/27/43/434002.
[174] M. Baibarac, T. Burlanescu, M. Stroe, I. Smaranda, C. Negrila, The Photoluminescence and Vibrational Properties of Black Phosphorous Sheets Chemically/Electrochemically Functionalized in the Presence of Diphenylamine, Polym. (Basel) 14 (2022), https://doi.org/10.3390/polym14214479.
[175] M.R. Molas, Ł. Macewicz, A. Wieloszyńska, P. Jakóbczyk, A. Wysmołek, R. Bogdanowicz, J.B. Jasinski, Photoluminescence as a probe of phosphorene properties, NPJ 2D Mater. Appl. 5 (2021), https://doi.org/10.1038/s41699-021-00263-8.
[176] Z.X. Gan, L.L. Sun, X.L. Wu, M. Meng, J.C. Shen, P.K. Chu, Tunable photoluminescence from sheet-like black phosphorus crystal by electrochemical oxidation, Appl. Phys. Lett. 107 (2015), https://doi.org/10.1063/1.4926727.
[177] H. Liu, H. Sung Choe, Y. Chen, J. Suh, C. Ko, S. Tongay, J. Wu, Variable range hopping electric and thermoelectric transport in anisotropic black phosphorus, Appl. Phys. Lett. 111 (2017), https://doi.org/10.1063/1.4985333.
[178] X. Ren, P. Lian, D. Xie, Y. Yang, Y. Mei, X. Huang, Z. Wang, X. Yin, Properties, preparation and application of black phosphorus/phosphorene for energy storage: a review, J. Mater. Sci. 52 (2017) 10364–10386, https://doi.org/10.1007/s10853-017-1194-3.
[179] M. Batmunkh, M. Bat-Erdene, J.G. Shapter, Phosphorene and phosphorene-based materials – prospects for future applications, Adv. Mater. 28 (2016) 8586–8617, https://doi.org/10.1002/adma.201602254.
[180] W. Zhang, X. Zhang, L.K. Ono, Y. Qi, H. Oughaddou, Recent advances in phosphorene: structure, synthesis, and properties, Small (2023), https://doi.org/10.1002/smll.202303115.
[181] P.V. Pham, S.C. Bodepudi, K. Shehzad, Y. Liu, Y. Xu, B. Yu, X. Duan, 2D Heterostructures for ubiquitous electronics and optoelectronics: principles, opportunities, and challenges, Chem. Rev. 122 (2022) 6514–6613, https://doi.org/10.1021/acs.chemrev.1c00735.
[182] M.S. Jayalakshmy, R.K. Mishra, Applications of carbon-based nanofiller-incorporated rubber composites in the fields of tire engineering, flexible electronics and EMI shielding, in: Carbon-Based Nanofillers and Their Rubber

Nanocomposites, Elsevier, 2019, pp. 441–472, https://doi.org/10.1016/B978-0-12-817342-8.00014-7.
[183] X. Bao, Properties of new two-dimensional nanomaterial black phosphorus, IOP Conf. Ser. Mater. Sci. Eng. 612 (2019) 022099, https://doi.org/10.1088/1757-899X/612/2/022099.
[184] J. Dai, X.C. Zeng, Bilayer phosphorene: effect of stacking order on bandgap and its potential applications in thin-film solar cells, J. Phys. Chem. Lett. 5 (2014) 1289–1293, https://doi.org/10.1021/jz500409m.
[185] A.H. Woomer, T.W. Farnsworth, J. Hu, R.A. Wells, C.L. Donley, S.C. Warren, Phosphorene: Synthesis, Scale-Up, and Quantitative Optical Spectroscopy, ACS Nano 9 (2015) 8869–8884, https://doi.org/10.1021/acsnano.5b02599.
[186] Y. Li, S. Yang, J. Li, Modulation of the Electronic Properties of Ultrathin Black Phosphorus by Strain and Electrical Field, J. Phys. Chem. C. 118 (2014) 23970–23976, https://doi.org/10.1021/jp506881v.
[187] X. Liu, C.R. Ryder, S.A. Wells, M.C. Hersam, Resolving the in-plane anisotropic properties of black phosphorus, Small Methods 1 (2017) 1700143, https://doi.org/10.1002/smtd.201700143.
[188] D. Grasseschi, D.A. Bahamon, F.C.B. Maia, A.H.C. Neto, R.O. Freitas, C.J.S. de Matos, Oxygen impact on the electronic and vibrational properties of black phosphorus probed by synchrotron infrared nanospectroscopy, 2d Mater. 4 (2017) 035028, https://doi.org/10.1088/2053-1583/aa8210.
[189] Y. Zhang, C. Ma, J. Xie, H. Ågren, H. Zhang, Black phosphorus/polymers: status and challenges, Adv. Mater. 33 (2021), https://doi.org/10.1002/adma.202100113.
[190] C. Chowdhury, A. Datta, Exotic physics and chemistry of two-dimensional phosphorus: phosphorene, J. Phys. Chem. Lett. 8 (2017) 2909–2916, https://doi.org/10.1021/acs.jpclett.7b01290.
[191] D. Scelta, A. Baldassarre, M. Serrano-Ruiz, K. Dziubek, A.B. Cairns, M. Peruzzini, R. Bini, M. Ceppatelli, The p-sc structure in phosphorus: Bringing order to the high pressure phases of group 15 elements, Chem. Commun. 54 (2018), https://doi.org/10.1039/c8cc03013h.
[192] R.K. Mishra, A. Kumar, Advanced biopolymer-based composites: An introduction and fracture modeling, 2021. ⟨https://doi.org/10.1016/B978-0-12-822291-1.00001-4⟩.
[193] R.K. Mishra, S. Goel, I. Chianella, H. Yazdani Nezhad, Graphene nanoplatelets/barium titanate polymer nanocomposite fibril: a remanufactured multifunctional material with unprecedented electrical, thermomechanical, and electromagnetic properties, Adv. Sustain Syst. 7 (2023), https://doi.org/10.1002/adsu.202300177.
[194] S. Moschetto, F. Prescimone, M. Bolognesi, S. Toffanin, Smart synthetic and surface-engineering approaches to functionalize 2d black phosphorus for real-setting applications, Adv. Mater. Interfaces 9 (2022), https://doi.org/10.1002/admi.202102149.
[195] Y. Yi, X.-F. Yu, W. Zhou, J. Wang, P.K. Chu, Two-dimensional black phosphorus: Synthesis, modification, properties, and applications, Mater. Sci. Eng.: R: Rep. 120 (2017) 1–33, https://doi.org/10.1016/j.mser.2017.08.001.
[196] D.W. Boukhvalov, A.N. Rudenko, D.A. Prishchenko, V.G. Mazurenko, M. I. Katsnelson, Chemical modifications and stability of phosphorene with impurities: A first principles study, Phys. Chem. Chem. Phys. 17 (2015), https://doi.org/10.1039/c5cp01901j.
[197] A.A. Kistanov, A.R. Davletshin, S.V. Ustiuzhanina, I. Evazzade, D. Saadatmand, S. V. Dmitriev, E.A. Korznikova, Effects of substrate and environmental adsorbates on the electronic properties and structural stability of antimonene, J. Mater. Sci. 53 (2018), https://doi.org/10.1007/s10853-018-2709-2.
[198] S. Qiu, B. Zou, T. Zhang, X. Ren, B. Yu, Y. Zhou, Y. Kan, Y. Hu, Integrated effect of NH2-functionalized/triazine based covalent organic framework black phosphorus on reducing fire hazards of epoxy nanocomposites, Chem. Eng. J. 401 (2020), https://doi.org/10.1016/j.cej.2020.126058.
[199] R.K. Mishra, S.K. Tiwari, S. Mohapatra, S. Thomas, Efficient Nanocarriers for Drug-Delivery Systems, in: Nanocarriers for Drug Delivery, Elsevier, 2019, pp. 1–41, https://doi.org/10.1016/B978-0-12-814033-8.00001-1.
[200] Raghvendra kumar Mishra, An Overview on Li-S Battery and Its Challenges, in: Applied Physical Chemistry with Multidisciplinary Approaches, 1st ed., Apple Academic Press Inc. CRC Taylor francis, 2018, pp. 136–153.
[201] F. Parveen, R. Kumar Mishra, Different Fabrication Techniques of Aerogels and Its Applications, in: Advanced Polymeric Materials for Sustainability and Innovations, 2019. ⟨https://doi.org/10.1201/b22326-14⟩.
[202] S. Qiu, Y. Zhou, X. Zhou, T. Zhang, C. Wang, R.K.K. Yuen, W. Hu, Y. Hu, Air-Stable Polyphosphazene-Functionalized Few-Layer Black Phosphorene for Flame Retardancy of Epoxy Resins, Small 15 (2019), https://doi.org/10.1002/smll.201805175.
[203] I. Shirotani, Growth of large single crystals of black phosphorus at high pressures and temperatures, and its electrical properties, Mol. Cryst. Liq. Cryst. 86 (1982) 203–211, https://doi.org/10.1080/00268948208073686.
[204] Y. Maruyama, S. Suzuki, K. Kobayashi, S. Tanuma, Synthesis and some properties of black phosphorus single crystals, Phys. B+C. 105 (1981) 99–102, https://doi.org/10.1016/0378-4363(81)90223-0.
[205] X. Ren, Y. Mei, P. Lian, D. Xie, W. Deng, Y. Wen, Y. Luo, Fabrication and application of black phosphorene/graphene composite material as a flame retardant, Polym. (Basel) 11 (2019), https://doi.org/10.3390/polym11020193.
[206] C. Su, H. Zhong, H. Chen, Y. Guo, Z. Guo, D. Huang, W. Zhang, Q. Wu, B. Yang, Z. Liu, Black phosphorus-polypyrrole nanocomposites for high-performance photothermal cancer therapy, N. J. Chem. 43 (2019), https://doi.org/10.1039/c9nj01249d.
[207] A. Kumar, Controlled nanostructures and simultaneous passivation of black phosphorus (phosphorene) with Nafion, J. Mater. Res 35 (2020), https://doi.org/10.1557/jmr.2019.395.
[208] R. Gusmão, Z. Sofer, M. Pumera, Black Phosphorus Rediscovered: From Bulk Material to Monolayers, Angew. Chem. Int. Ed. 56 (2017) 8052–8072, https://doi.org/10.1002/anie.201610512.
[209] M. Batmunkh, M. Bat-Erdene, J.G. Shapter, Black Phosphorus: Synthesis and Application for Solar Cells, Adv. Energy Mater. 8 (2018), https://doi.org/10.1002/aenm.201701832.
[210] R.K. Mishra, A. Shaji, S. Thomas, Processing, rheology, barrier properties, and theoretical study of microfibrillar and nanofibrillar in situ composites, 2017. ⟨https://doi.org/10.1016/B978-0-08-101991-7.00010-8⟩.
[211] R. Km, S. L, Fabrication Techniques of Micro/Nano Fibres based Nonwoven Composites: A Review, Mod. Chem. Appl. 05 (2017), https://doi.org/10.4172/2329-6798.1000206.
[212] V.V. Kulish, O.I. Malyi, C. Persson, P. Wu, Phosphorene as an anode material for Na-ion batteries: A first-principles study, Phys. Chem. Chem. Phys. 17 (2015), https://doi.org/10.1039/c5cp01502b.
[213] M. Bolognesi, M. Brucale, A. Lorenzoni, F. Prescimone, S. Moschetto, V. V. Korolkov, M. Baldoni, M. Serrano-Ruiz, M. Caporali, F. Mercuri, E. Besley, M. Muccini, M. Peruzzini, P.H. Beton, S. Toffanin, Epitaxial multilayers of alkanes on two-dimensional black phosphorus as passivating and electrically insulating nanostructures, Nanoscale 11 (2019), https://doi.org/10.1039/c9nr01155b.
[214] A. Pon, A. Bhattacharyya, R. Rathinam, Recent Developments in Black Phosphorous Transistors: A Review, J. Electron Mater. 50 (2021), https://doi.org/10.1007/s11664-021-09183-1.
[215] J. Liu, Y. Zhou, W. Zhu, Determining bandgap of black phosphorus using capacitance, Appl. Phys. Lett. 116 (2020), https://doi.org/10.1063/5.0010165.
[216] A. Castellanos-Gomez, Black Phosphorus: Narrow Gap, Wide Applications, J. Phys. Chem. Lett. 6 (2015), https://doi.org/10.1021/acs.jpclett.5b01686.
[217] K. Wang, Z. He, X. Li, K. Xu, Q. Zhou, X. Ye, T. Zhang, S. Jiang, Y. Zhang, B. Hu, C. Chen, Black-phosphorus-based junctions and their optoelectronic device applications, Nano Res 16 (2023), https://doi.org/10.1007/s12274-022-5008-9.
[218] F. Telesio, G. Le Gal, M. Serrano-Ruiz, F. Prescimone, S. Toffanin, M. Peruzzini, S. Heun, Ohmic contact engineering in few-layer black phosphorus: Approaching the quantum limit, Nanotechnology 31 (2020), https://doi.org/10.1088/1361-6528/ab8cf4.
[219] A. Jain, A.J.H. McGaughey, Strongly anisotropic in-plane thermal transport in single-layer black phosphorene, Sci. Rep. 5 (2015), https://doi.org/10.1038/srep08501.
[220] D. Lee, Y. Choi, E. Hwang, M.S. Kang, S. Lee, J.H. Cho, Black phosphorus nonvolatile transistor memory, Nanoscale 8 (2016), https://doi.org/10.1039/c6nr02078j.
[221] S. Moschetto, M. Bolognesi, F. Prescimone, M. Brucale, A. Mezzi, L. Ortolani, M. Caporali, P. Pingue, M. Serrano-Ruiz, D. Pisignano, M. Peruzzini, L. Persano, S. Toffanin, Large-Area Oxidized Phosphorene Nanoflakes Obtained by Electrospray for Energy-Harvesting Applications, ACS Appl. Nano Mater. 4 (2021), https://doi.org/10.1021/acsanm.0c03465.
[222] Y.-y Carpenter, T. Baumgartner, Phosphorus-Containing Polymers, in: Comprehensive Inorganic Chemistry II, Elsevier, 2013, pp. 893–932, https://doi.org/10.1016/B978-0-08-097774-4.00131-5.
[223] H. Mu, S. Lin, Z. Wang, S. Xiao, P. Li, Y. Chen, H. Zhang, H. Bao, S.P. Lau, C. Pan, D. Fan, Q. Bao, Black phosphorus–polymer composites for pulsed lasers, Adv. Opt. Mater. 3 (2015) 1447–1453, https://doi.org/10.1002/adom.201500336.
[224] P. Lun, Z. Chen, Z. Zhang, S. Tan, D. Chen, Enhanced ionic conductivity in halloysite nanotube-poly(vinylidene fluoride) electrolytes for solid-state lithium-ion batteries, RSC Adv. 8 (2018) 34232–34240, https://doi.org/10.1039/C8RA06856A.
[225] M. Ulaganathan, S. Rajendran, Novel Li-ion conduction on poly(vinyl acetate)-based hybrid polymer electrolytes with double plasticizers, J. Appl. Electrochem 41 (2011) 83–88, https://doi.org/10.1007/s10800-010-0211-x.
[226] B.N. Choi, J.H. Yang, Y.S. Kim, C.-H. Chung, Effect of morphological change of copper-oxide fillers on the performance of solid polymer electrolytes for lithium-metal polymer batteries, RSC Adv. 9 (2019) 21760–21770, https://doi.org/10.1039/C9RA03555A.
[227] S. Kim, J. Cui, V.P. Dravid, K. He, Orientation-Dependent Intercalation Channels for Lithium and Sodium in Black Phosphorus, Adv. Mater. 31 (2019), https://doi.org/10.1002/adma.201904623.
[228] W. Zheng, J. Lee, Z. Gao, Y. Li, S. Lin, S.P. Lau, L.Y.S. Lee, Laser-assisted ultrafast exfoliation of black phosphorus in liquid with tunable thickness for Li-ion batteries, Adv. Energy Mater. 10 (2020), https://doi.org/10.1002/aenm.201903490.
[229] W. Xu, K.S. Siow, Z. Gao, S.Y. Lee, Ionic conductivity and electrochemical characterization of novel microporous composite polymer electrolytes, J. Electrochem Soc. 146 (1999) 4410–4418, https://doi.org/10.1149/1.1392652.
[230] S. Kim, J. Cui, V.P. Dravid, K. He, Orientation-Dependent Intercalation Channels for Lithium and Sodium in Black Phosphorus, Adv. Mater. 31 (2019), https://doi.org/10.1002/adma.201904623.
[231] R. Kumar Mishra, T. Eren, D.-Y. Wang, Inorganic polymers as flame-retardant materials, 2019. ⟨https://doi.org/10.1002/9783527819140.ch8⟩.
[232] Y. Tang, K. Yang, Z. Hua, F. Yin, W. Yuan, A new sensing material design based on chemically passivated phosphorene/porous two-dimensional polymer: Highly sensitive and selective detection of NO2, Sens Actuators B Chem. 329 (2021), https://doi.org/10.1016/j.snb.2020.129233.
[233] Z. Li, Q. Liu, S. Tang, D. Feng, W. Zhao, B. Li, D. Xie, Y. Mei, Dual modification of EVA by long chain phosphaphenanthrene grafted MXene and black phosphorene

nanosheets for simultaneously enhanced thermal stability and flame retardancy, Colloids Surf. A Physicochem Eng. Asp. 664 (2023), https://doi.org/10.1016/j.colsurfa.2023.131198.
[234] F. Shi, B. Wang, L. Yan, B. Wang, Y. Niu, L. Wang, W. Sun, In-situ growth of nitrogen-doped carbonized polymer dots on black phosphorus for electrochemical DNA biosensor of Escherichia coli O157: H7, Bioelectrochemistry 148 (2022), https://doi.org/10.1016/j.bioelechem.2022.108226.
[235] R.K. Mishra, R. Rajakumari, Nanobiosensors Biomed. Appl. (2018), https://doi.org/10.1016/B978-0-12-814031-4.00001-5.
[236] Z. Qu, K. Wu, E. Jiao, W. Chen, Z. Hu, C. Xu, J. Shi, S. Wang, Z. Tan, Surface functionalization of few-layer black phosphorene and its flame retardancy in epoxy resin, Chem. Eng. J. 382 (2020), https://doi.org/10.1016/j.cej.2019.122991.
[237] Z. Qu, K. Wu, W. Meng, B. Nan, Z. Hu, C. An Xu, Z. Tan, Q. Zhang, H. Meng, J. Shi, Surface coordination of black phosphorene for excellent stability, flame retardancy and thermal conductivity in epoxy resin, Chem. Eng. J. 397 (2020), https://doi.org/10.1016/j.cej.2020.125416.
[238] G. Tiouitchi, M. Raji, O. Mounkachi, M.A. Ali, A. Mahmoud, F. Boschini, H. Essabir, R. Bouhfid, A. El kacem Qaiss, Black phosphorus-based polyvinylidene fluoride nanocomposites: Synthesis, processing and characterization, Compos B Eng. 175 (2019), https://doi.org/10.1016/j.compositesb.2019.107165.
[239] R.K. Mishra, S.T. Abdulrahman, Tribological performance of polymer composite materials, in: N.S.K.S.T. Didier Rouxel (Ed.), Advanced Polymeric Materials: Synthesis and Applications, 1st ed., River Publishers, 2022, pp. 193–246.
[240] T.H. Wang, T.K.A. Nguyen, R. An Doong, Phosphorene nanosheet decorated graphitic carbon nitride nanofiber for photoelectrochemically enhanced hydrogen evolution from water splitting, J. Taiwan Inst. Chem. Eng. 141 (2022), https://doi.org/10.1016/j.jtice.2022.104577.
[241] L. He, X. Zhou, W. Cai, Y. Xiao, F. Chu, X. Mu, X. Fu, Y. Hu, L. Song, Electrochemical exfoliation and functionalization of black phosphorene to enhance mechanical properties and flame retardancy of waterborne polyurethane, Compos B Eng. 202 (2020) 108446, https://doi.org/10.1016/j.compositesb.2020.108446.
[242] B. Zou, S. Qiu, P. Jia, X. Jiang, L. Song, Y. Hu, Photothermal and fire-safe epoxy/black phosphorene composites: Molecular structure analysis of sutured char, Appl. Surf. Sci. 605 (2022), https://doi.org/10.1016/j.apsusc.2022.154848.
[243] Z. Qu, C. An Xu, Z. Hu, Y. Li, H. Meng, Z. Tan, J. Shi, K. Wu, (CF3SO3)3Er-decorated black phosphorene for robust ambient stability and excellent flame retardancy in epoxy resin, Compos B Eng. 202 (2020), https://doi.org/10.1016/j.compositesb.2020.108440.
[244] Y. Luo, Y. Xie, W. Geng, J. Chu, H. Wu, D. Xie, X. Sheng, Y. Mei, Boosting fire safety and mechanical performance of thermoplastic polyurethane by the face-to-face two-dimensional phosphorene/MXene architecture, J. Mater. Sci. Technol. 129 (2022), https://doi.org/10.1016/j.jmst.2022.05.003.
[245] L. He, X. Jiang, X. Zhou, Z. Li, F. Chu, X. Wang, W. Cai, L. Song, Y. Hu, Integration of black phosphorene and MXene to improve fire safety and mechanical properties of waterborne polyurethane, Appl. Surf. Sci. 581 (2022), https://doi.org/10.1016/j.apsusc.2021.152386.
[246] W. Yang, S. Qiu, Y. Zhou, J. Wang, B. Zou, L. Song, Covalent grafting diazotized black phosphorus with ferrocene oligomer towards smoke suppression and toxicity reduction, Chemosphere 303 (2022), https://doi.org/10.1016/j.chemosphere.2022.135012.
[247] R. Mishra, M.K. Aswathi, S. Thomas, CHAPTER 7: High Performance Flooring Materials from Recycled Rubber, 2019. ⟨https://doi.org/10.1039/9781788013482-00160⟩.
[248] S. Yin, X. Ren, R. Zheng, Y. Li, J. Zhao, D. Xie, Y. Mei, Improving fire safety and mechanical properties of waterborne polyurethane by montmorillonite-passivated black phosphorus, Chem. Eng. J. 464 (2023), https://doi.org/10.1016/j.cej.2023.142683.
[249] R.K. Mishra, J. Abraham, K. Joseph, K. Jayanarayanan, N. Kalarikkal, S. Thomas, Conduct. Polyurethane Compos. (2017), https://doi.org/10.1016/B978-0-12-804065-2.00012-7.
[250] M. Ghambarian, Z. Azizi, M. Ghashghaee, Phosphorene defects for high-quality detection of nitric oxide and carbon monoxide: A periodic density functional study, Chem. Eng. J. 396 (2020), https://doi.org/10.1016/j.cej.2020.125247.
[251] Y.K. Kim, Y. Lee, K.Y. Shin, Black phosphorus-based smart electrorheological fluid with tailored phase transition and exfoliation, J. Ind. Eng. Chem. 90 (2020), https://doi.org/10.1016/j.jiec.2020.07.032.
[252] R.K. Mishra, D. Li, I. Chianella, S. Goel, S. Lotfian, H.Y. Nezhad, Electric field induced extrinsic strains in BaTiO3-epoxy nanocomposite: a contact-less mechanical property tailoring smart material, Res Sq. (2022), https://doi.org/10.21203/rs.3.rs-2331217/v1.
[253] Z. Zhang, Y. Li, J. Xu, Y. Wen, Electropolymerized molecularly imprinted polypyrrole decorated with black phosphorene quantum dots onto poly(3,4-ethylenedioxythiophene) nanorods and its voltammetric sensing of vitamin C, J. Electroanal. Chem. 814 (2018), https://doi.org/10.1016/j.jelechem.2018.02.059.
[254] W. Aftab, M. Khurram, S. Jinming, H. Tabassum, Z. Liang, A. Usman, W. Guo, X. Huang, W. Wu, R. Yao, Q. Yan, R. Zou, Highly efficient solar-thermal storage coating based on phosphorene encapsulated phase change materials, Energy Storage Mater. 32 (2020), https://doi.org/10.1016/j.ensm.2020.07.032.
[255] G. Yanalak, F. Doganay, Z. Eroglu, H. Kucukkececi, E. Aslan, M. Ozmen, S.Z. Bas, O. Metin, I. Hatay Patir, Ternary nanocomposites of mesoporous graphitic carbon nitride/black phosphorus/gold nanoparticles (mpg-CN/BP-Au) for photocatalytic hydrogen evolution and electrochemical sensing of paracetamol, Appl. Surf. Sci. 557 (2021), https://doi.org/10.1016/j.apsusc.2021.149755.
[256] T. Xue, Y. Sheng, J. Xu, Y. Li, X. Lu, Y. Zhu, X. Duan, Y. Wen, In-situ reduction of Ag+ on black phosphorene and its NH2-MWCNT nanohybrid with high stability and dispersibility as nanozyme sensor for three ATP metabolites, Biosens. Bioelectron. 145 (2019), https://doi.org/10.1016/j.bios.2019.111716.
[257] S. Yılmaz, E.G. Acar, G. Yanalak, E. Aslan, M. Kılıç, İ. Hatay Patır, Ö. Metin, Enhanced hydrogen evolution by using ternary nanocomposites of mesoporous carbon nitride/black phosphorous/transition metal nanoparticles (m-gCN/BP-M; M = Co, Ni, and Cu) as photocatalysts under visible light: A comparative experimental and theoretical study, Appl. Surf. Sci. 593 (2022), https://doi.org/10.1016/j.apsusc.2022.153398.
[258] X. Zhu, L. Lin, R. Wu, Y. Zhu, Y. Sheng, P. Nie, P. Liu, L. Xu, Y. Wen, Portable wireless intelligent sensing of ultra-trace phytoregulator α-naphthalene acetic acid using self-assembled phosphorene/Ti3C2-MXene nanohybrid with high ambient stability on laser induced porous graphene as nanozyme flexible electrode, Biosens. Bioelectron. 179 (2021), https://doi.org/10.1016/j.bios.2021.113062.
[259] M.S. Kang, S.J. Song, J.H. Cha, Y. Cho, H.U. Lee, S.H. Hyon, J.H. Lee, D.W. Han, Increased neuritogenesis on ternary nanofiber matrices of PLCL and laminin decorated with black phosphorus, J. Ind. Eng. Chem. 92 (2020), https://doi.org/10.1016/j.jiec.2020.09.009.
[260] Y. Wang, Y. Zhou, Y. Wang, R. Zhang, J. Li, X. Li, Z. Zang, Conductometric room temperature ammonia sensors based on titanium dioxide nanoparticles decorated thin black phosphorus nanosheets, Sens Actuators B Chem. 349 (2021), https://doi.org/10.1016/j.snb.2021.130770.
[261] Z. Liu, K. Liu, R. Sun, J. Ma, Biorefinery-assisted ultra-high hydrogen evolution via metal-free black phosphorus sensitized carbon nitride photocatalysis, Chem. Eng. J. 446 (2022), https://doi.org/10.1016/j.cej.2022.137128.
[262] N. Li, R. Wang, C. Wang, J. Gao, Z. Liu, J. Gu, T. Jiao, Self-assembled photo-responsive black phosphorus-azobenzene composite Langmuir films with chemical gas sensor and photoelectric conversion applications, Colloids Surf. A Physicochem Eng. Asp. 624 (2021), https://doi.org/10.1016/j.colsurfa.2021.126811.
[263] C. Xue, L. Sutrisno, M. Li, W. Zhu, Y. Fei, C. Liu, X. Wang, K. Cai, Y. Hu, Z. Luo, Implantable multifunctional black phosphorus nanoformulation-deposited biodegradable scaffold for combinational photothermal/ chemotherapy and wound healing, Biomaterials 269 (2021), https://doi.org/10.1016/j.biomaterials.2020.120623.
[264] S.B. Prasanna, Y.C. Lin, S.K. Ramaraj, U. Dhawan, X. Liu, C.W. Tung, R. Sakthivel, R.J. Chung, 2D/2D heterostructure Ni-Fe LDH/black phosphorus nanosheets with AuNP for noxious substance diphenylamine detection in food samples, Food Chem. 432 (2024), https://doi.org/10.1016/j.foodchem.2023.137295.
[265] J. Liu, P. Du, T. Liu, B.J. Córdova Wong, W. Wang, H. Ju, J. Lei, A black phosphorus/manganese dioxide nanoplatform: Oxygen self-supply monitoring, photodynamic therapy enhancement and feedback, Biomaterials 192 (2019), https://doi.org/10.1016/j.biomaterials.2018.10.018.